

FEDLOC: FEDERATED LEARNING FRAMEWORK FOR COOPERATIVE LOCALIZATION AND LOCATION DATA PROCESSING

Feng Yin^{*1}, Zhidi Lin¹, Yue Xu², Qinglei Kong¹, Deshi Li³, Sergios Theodoridis¹, Shuguang (Robert) Cui¹

1. The Chinese University of Hong Kong (Shenzhen) and SRIBD, 518172, China
2. BeiJing University of Post and Telecommunications
3. Wuhan University

ABSTRACT

In this paper, we propose a new localization framework in which mobile users or smart agents can cooperate to build accurate location services without sacrificing privacy, in particular, information related to their trajectories. The proposed framework is called *Federated Localization (FedLoc)*, simply because it adopts the recently proposed federated learning. Apart from the new *FedLoc* framework, this paper can be deemed as an *overview paper*, in which we review the state-of-the-art federated learning framework, two widely used learning models, various distributed model hyper-parameter optimization schemes, and some practical use cases that fall under the *FedLoc* framework. The use cases, summarized from a mixture of standard, recently published, and unpublished works, cover a broad range of location services, including collaborative static localization/fingerprinting, indoor target tracking, outdoor navigation using low-sampling GPS, and spatio-temporal wireless traffic data modeling and prediction. The obtained primary results confirm that the proposed FedLoc framework well suits data-driven, machine learning-based localization and spatio-temporal data modeling. Future research directions are discussed at the end of this paper.

Index Terms— Cooperation, Data-driven learning models, Distributed processing, Federated Learning, Gaussian Processes, Localization, Location services, User privacy.

1. INTRODUCTION

With the explosion of data and the ever-increasing computing power, we have witnessed nowadays the popularity of machine learning models and algorithms which are data-driven. Principally, with more data, a complicated underlying system/dynamic/regression function can be modeled more accurately. However, when the data size increases beyond a limit, the scale of the model and the computational complexity of an associated learning algorithm become huge. For instance, Gaussian process models scale cubically with the data size [1].

The recently proposed federated learning framework [2] has received a lot of attention, as it enables a large-scale machine learning model to be trained jointly by collaborations

of a large number of mobile users. Actually, there exist various similar work before the federated learning, for instance [3, 4], but the new framework emphasizes more on the following aspects: (1) non-i.i.d. data; (2) unbalanced local data size; (3) large number of local users; (4) limited communication; and (5) data privacy [2]. It deserves to highlight that federated learning is a promising technical solution to solve the ever-increasing concerns about the loss of privacy data and information and to meet the ever-stringent data protection regulations world-wide, for instance, the General Data Protection Regulation (GDPR) implemented by the European Union in 2018. Federated learning has triggered various potential applications in the sectors of smart medicine, finance, and next-generation wireless communications [5, 6, 7]. In this paper, we extend federated learning to a new application sector, namely target localization and location-related services.

Target localization is meant to provide an estimate of the desired position as accurate as possible. There exist already a plethora of techniques for static target localization, target tracking, navigation, interested readers can refer to [8, 9, 10] and their references for more information. Most of these techniques rely on empirical, parametric transition and measurement models, which can be regarded as individual abstract of human experience, thus may severely mismatch the underlying mechanism in complicated environments such as office, shopping mall, museum, etc. However, directly learning from a huge volume of historical data may help to alleviate such model mismatch and improve the positioning accuracy even further. Apart from the traditional localization, a new type of location services emerged in the recent years under the umbrella of smart city, namely the spatio-temporal location data prediction. This type of services include but not limited to wireless traffic prediction, taxi supply and demand prediction, energy consumption prediction, air pollution prediction at specific locations. Data-driven, learning model based solutions have demonstrated great data representation capability and provided outstanding data prediction performance [11, 12, 13, 14].

However, the greatest difficulty that we confronted when applying machine learning models to localization and location data modeling lies in the big amount of training data

required, which can be easily resolved by cooperation through aggregating raw data collected from a big number of mobile users yet may cause data privacy issue as a consequence. The federated learning framework is an outstanding solution for enhancing wireless localization accuracy and maintaining safe cooperation among users at the same time.

The gist of the proposed Federated Localization (FedLoc) framework is that each mobile user/smart agent collects a smaller scale, local data set and approximates the global machine learning model in a cooperative manner. Some concrete examples are as follows: (1) For static localization, the mobile users collect radio features at specific positions obtained from global positioning system (GPS) (for outdoor scenarios) or from the proximity to indoor reference points/landmarks (for indoor scenarios); (2) For target tracking and navigation, the mobile users collect diverse trajectories of sensor and wireless observations; (3) For wireless traffic prediction, the smart agents collect local wireless data usage generated by the serving mobile users. We believe that the FedLoc framework is an up-and-coming solution for futuristic data-driven cooperative localization, not only because of the rapid development of distributed optimization techniques that serve as the algorithmic core, but also largely owing to the rapid development of smart phones with ever-increasing computation power and network throughput, the widespread use of quick-response (QR) codes, and the high-precision indoor/outdoor maps, altogether. Therefore, we believe it is timely to propose the idea of federated localization and location data processing.

The contributions of this paper are as follows.

- First, we proposed a novel federated localization framework, short as FedLoc, which elegantly addresses the privacy issue in cooperation among a massive number of mobile users for target localization and location data processing. Two potential wireless network infrastructures that can potentially support the communication requirements of the FedLoc framework are also discussed.
- Second, we clearly clarified the differences between the proposed FedLoc framework and the existing cooperative localization framework for sensor network as well as the classic crowdsourcing framework.
- Third, we reviewed some state-of-the-art federated learning procedures, two widely used learning models, namely the deep neural network (DNN) and Gaussian process (GP), and a few distributed model hyperparameter optimization schemes that work reasonably well for the two learning models. We put a bit more emphasis on the GP models due to their unique welcome features that make them more suitable to use than DNN for location data.
- Fourth, we give four concrete use cases, namely (1) static target localization; (2) outdoor vehicle navigation;

(3) indoor pedestrian motion tracking; and (4) spatio-temporal wireless traffic prediction, to explain the use of the FedLoc framework. In the first use case, a static target localization system is built based on DNN that maps a vector of radio features to a desired position. In the second use case, we proposed a DNN based accurate vehicle navigation with low-sampling-rate GPS. In the third case, state transition function as represented by the GP model maps the current state to the next state in a non-parametric way for indoor pedestrian motion modeling. In the fourth use case, wireless traffic is modeled by a scalable GP under 5G Cloud-Radio Access Network (C-RAN) infrastructure. Various other related applications are also mentioned briefly.

- Fifth, we evaluated the proposed FedLoc framework all with real data sets for the aforementioned use cases to demonstrate its effectiveness.

In this review paper, we concentrate on federated learning tailored to target localization and location data processing. Due to the space limitation as well as the expertise of the authors, the following parts are only briefly touched upon.

- Due to the rapid development of distributed optimization methods in the contexts of robustness, communication efficiency, and low-complexity, etc., we are unable to give a timely survey of all recent advances. But we strongly believe that a majority of these advanced methods can be used to enhance our FedLoc framework even further.
- Encryption and decryption schemes are considered for federated learning to large extent nowadays. In this paper, we only gave a brief survey of the state-of-the-art schemes. While the most recent and advanced works, for instance the block-chain based scheme, is outside the scope of this review paper.

The rest of this paper is organized as follows. In Section 2, we briefly review the existing “cooperation” framework considered primarily for wireless sensor networks. In Section 3, we introduce two important learning models, namely the deep neural networks and Gaussian processes, for learning from data. In Section 4, we introduce the proposed FedLoc framework in detail, followed by two potential wireless network infrastructures given in Section 5 that support the proposed FedLoc framework in real scenarios. Various use cases of the proposed FedLoc framework are showcased in Section 6. Simulation results are given in Section 7 to demonstrate the effectiveness of the FedLoc framework. In Section 8, we discuss the major challenges of the FedLoc framework and give a few future research directions. Lastly, Section 9 concludes this paper.

2. RELATED WORK

In this section, we survey the existing frameworks for cooperative localization and clarify their differences with the FedLoc framework proposed by us in Section 4.

2.1. Sensor Network Localization

When speaking of “cooperation” in the context of wireless localization, it will certainly remind us the class of algorithms for determining a number of agents (nodes with unknown positions) with the aid of a few anchors (nodes with known positions) and a bunch of wireless measurements made between these nodes.

Cooperative localization has gained much attention since 2005 owing to the seminal work by Patwari and Hero [15], where they proposed to use the simple least-squares estimation criterion with time-of-arrival (ToA) or received-signal-strength (RSS) measurements to localize dozens of agents. The proposed method was evaluated with two sets of real measurements collected in an indoor environment. This seminal work has triggered a plethora of methods in the following years. Representative works include [16, 17], to mention a few.

The fundamental differences between the aforementioned cooperative localization algorithms and our proposed FedLoc are the following:

- In the above mentioned cooperative localization algorithms, the agents (could be a wireless sensor, a robot, or a mobile user) work together to determine their own positions. While in the new proposed FedLoc framework, the mobile users cooperate to train a global, learning-based model that will be used later in the online phase to predict novel positions upon request.
- The above mentioned cooperative localization adopts empirical models, such as the log-distance path-loss model for RSS measurements [18], and Gaussian mixture model for non-line-of-sight propagation [19]. While in the FedLoc framework, we solely consider data-driven, machine learning-based models.

2.2. Crowdsourcing

According to Wikipedia, Crowdsourcing is a sourcing model in which services are built from a large, relatively open, and often rapidly-evolving group of internet users. Building and maintaining a location system/service based on crowdsourcing is somewhat related to our FedLoc idea. However, the state-of-the-art crowdsourcing methods place more emphasis on raw data sharing and aggregation from a bunch of collaborating users, and normally there is no model in mind; even if there is a model assumed, it remains simple and heuristic. Representative works are as follows. In geography, voluntary users collaboratively build a street map, fill in street information, etc. OpenStreetMap (<http://www.openstreetmap.com>)

and Wikimapia (<http://www.wikimapia.org>) are two successful crowdsourcing projects among others. Crowdsourcing of virtual maps, such as RSS map or magnetic map, etc. becomes trendy for big multi-storey buildings [20, 21].

The fundamental differences between the crowdsourcing based localization and our FedLoc are the following:

- Crowdsourcing is more about raw location data aggregation for map construction with less calibration effort, while position determination will be done in a separate stage later on. In contrast, FedLoc focuses on training a global machine learning model for positioning in one step.
- Crowdsourcing is mostly model-free. In contrast, FedLoc is built around advanced machine learning models, making it more diverse.
- Crowdsourcing merely aggregates raw data without protections, such as data desensitization and encryption, which will incur severe privacy issues. In contrast, FedLoc processes sensitive data locally and exchanges only the model hyper-parameters that are difficult to decode in general.

3. LEARNING MODELS

Thanks to the big data, powerful computing facilities, and algorithmic innovations all together, we have witnessed in the past five years the great success of learning models in numerous applications, among others, image recognition, computer vision, and natural language processing. This section aims to introduce two representative learning models that can be used as the “brain” of the proposed FedLoc framework. We will first briefly review the deep neural network (DNN) models in Subsection 3.1, followed by a short introduction on Gaussian process (GP) models in Subsection 3.2. Lastly, we will shed some light on the connections of the two learning models and further highlight the benefits of using GP models over DNN models for FedLoc in Subsection 3.3.

3.1. Deep Neural Network

The deep neural network refers here the class of feedforward networks or multilayer perceptrons. The development of the neural networks is largely inspired by the neuroscience. An artificial DNN often demonstrates a chain structure, in math as: $f(\mathbf{x}) = f^{(L+1)}(\dots f^3(f^{(2)}(f^{(1)}(\mathbf{x}; \mathbf{W}_1); \mathbf{W}_2); \mathbf{W}_3); \mathbf{W}_{L+1})$, starting from the inputs/features \mathbf{x} and passing L hidden layers to the output eventually. In each hidden layer, the mapping function $f^{(i)}(\cdot)$ comprises a bunch of elementary activation functions that mimic the role of neurons of our brain. The commonly used activation functions include the sigmoid function, rectified linear unit (ReLU) function, and some other variants. The term feedforward means that data is fed from the

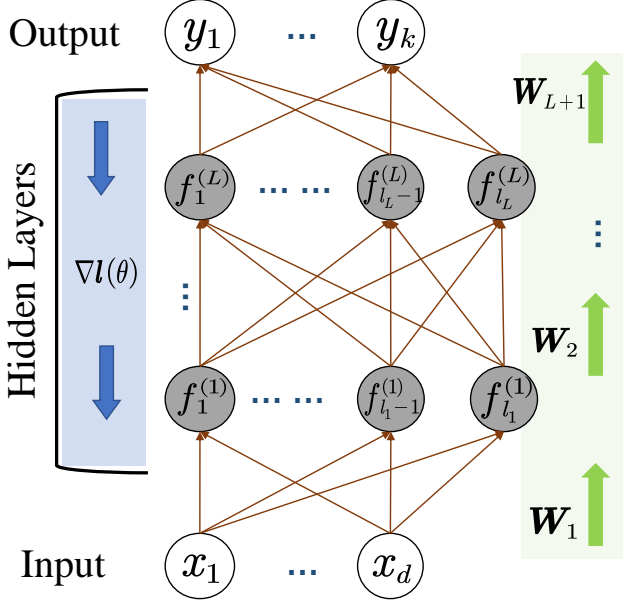


Fig. 1. Block diagram of deep neural network architecture. The input-, hidden-, and output variables are represented by nodes, and the weight parameters linking between the nodes at each layer are represented by the vector $\mathbf{W}_i, i \in [1, L + 1]$. $\boldsymbol{\theta} = \{\mathbf{W}_1, \mathbf{W}_2, \dots, \mathbf{W}_{L+1}\}$ is a vector of all model hyper-parameters, namely the neural network weights of all layers. Green arrows indicate the forward direction of information flow through the network in the inference stage, while the blue arrows indicate the backward direction of gradient flow for hyper-parameter optimization when using the back-propagation method.

input layer through several hidden layers to the output layer. According to the universal approximation theorem [22], a DNN can well approximate any smooth function by selecting the number of hidden layers and the number of neurons in each hidden layer. In order to train the hyper-parameters of a DNN, back-propagation algorithm is often adopted despite of its numerical problems, such as gradient vanishing and explosion. More details about DNN can be found in [23, 24].

3.2. Gaussian Process

Gaussian processes (GP) constitute an important class of Bayesian non-parametric models for machine learning which are closely related to several other popular models. A Gaussian process is a collection of random variables, any finite subset of which follows a Gaussian distribution [1]. In the sequel, we solely focus on scalar, real-valued Gaussian processes that are completely specified by a mean function and a kernel function (a.k.a. covariance function). Concretely,

$$f(\mathbf{x}) \sim \mathcal{GP}(m(\mathbf{x}), k(\mathbf{x}, \mathbf{x}'; \boldsymbol{\theta}_h)), \quad (1)$$

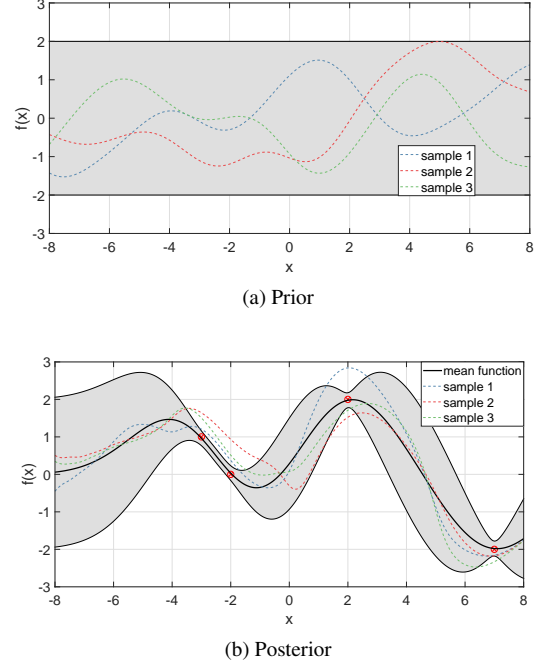


Fig. 2. Subfigure (a) shows three function samples drawn randomly from a GP prior with squared-exponential kernel. Subfigure (b) shows three random functions drawn from the posterior, i.e. the prior in (a) conditioned on the four noisy observations indicated by red dots. The corresponding posterior mean function is shown using the black curve. The grey shaded area represents the uncertainty area, namely the 95% confidence region for both the prior and the posterior, respectively.

where $m(\mathbf{x})$ is the mean function, which is often set to zero in practice, especially when there is no prior knowledge; and $k(\mathbf{x}, \mathbf{x}'; \boldsymbol{\theta}_h)$ is the kernel function tuned by the kernel hyper-parameters, $\boldsymbol{\theta}_h$.

Let us consider the following GP regression model

$$y = f(\mathbf{x}) + e, \quad (2)$$

where $y \in \mathbb{R}$ is a continuous-valued, scalar output; the unknown function $f(\mathbf{x}) : \mathbb{R}^d \mapsto \mathbb{R}$ is modeled as a zero mean GP; and the noise e is assumed to be Gaussian distributed with zero mean and variance σ_e^2 . Moreover, the noise terms at different data points are assumed to be mutually independent. The set of all unknown GP hyper-parameters is denoted by $\boldsymbol{\theta} \triangleq [\boldsymbol{\theta}_h^T, \sigma_e^2]^T$ and the dimension of $\boldsymbol{\theta}$ is assumed to be p .

The joint prior distribution of the training output \mathbf{y} and test output \mathbf{y}_* can be written as:

$$\begin{bmatrix} \mathbf{y} \\ \mathbf{y}_* \end{bmatrix} \sim \mathcal{N} \left(\mathbf{0}, \begin{bmatrix} \mathbf{K}(\mathbf{X}, \mathbf{X}) + \sigma_e^2 \mathbf{I}_n, & \mathbf{K}(\mathbf{X}, \mathbf{X}_*) \\ \mathbf{K}(\mathbf{X}_*, \mathbf{X}), & \mathbf{K}(\mathbf{X}_*, \mathbf{X}_*) + \sigma_e^2 \mathbf{I}_{n_*} \end{bmatrix} \right),$$

where $\mathbf{K}(\mathbf{X}, \mathbf{X})$ is an $n \times n$ covariance matrix between the training inputs; $\mathbf{K}(\mathbf{X}, \mathbf{X}_*)$ is an $n \times n_*$ covariance matrix

between the training inputs and test inputs, $\mathbf{K}(\mathbf{X}_*, \mathbf{X}_*)$ is an $n_* \times n_*$ covariance matrix between the test inputs.

- $\mathbf{K}(\mathbf{X}, \mathbf{X})$ is an $n \times n$ matrix of covariances among training inputs;
- $\mathbf{K}(\mathbf{X}, \mathbf{X}_*)$ is an $n \times n_*$ matrix of covariances between training inputs and test inputs; $\mathbf{K}(\mathbf{X}_*, \mathbf{X}) = \mathbf{K}(\mathbf{X}, \mathbf{X}_*)^T$;
- $\mathbf{K}(\mathbf{X}_*, \mathbf{X}_*)$ is an $n_* \times n_*$ matrix of covariances among test inputs.

Here, we let $\mathbf{K}(\mathbf{X}, \mathbf{X})$ be the short term of $\mathbf{K}(\mathbf{X}, \mathbf{X}; \theta_h)$.

Applying the results of conditional Gaussian distributions, we can easily derive the posterior distribution as

$$p(\mathbf{y}_* | \mathcal{D}, \mathbf{X}_*; \theta_h) \sim \mathcal{N}(\bar{\mathbf{m}}, \bar{\mathbf{V}}), \quad (3)$$

where the posterior mean (vector) and posterior covariance (matrix) are respectively,

$$\bar{\mathbf{m}} = \mathbf{K}(\mathbf{X}_*, \mathbf{X}) [\mathbf{K}(\mathbf{X}, \mathbf{X}) + \sigma_e^2 \mathbf{I}_n]^{-1} \mathbf{y}, \quad (4)$$

$$\begin{aligned} \bar{\mathbf{V}} &= \mathbf{K}(\mathbf{X}_*, \mathbf{X}_*) + \sigma_e^2 \mathbf{I}_{n_*} \\ &\quad - \mathbf{K}(\mathbf{X}_*, \mathbf{X}) [\mathbf{K}(\mathbf{X}, \mathbf{X}) + \sigma_e^2 \mathbf{I}_n]^{-1} \mathbf{K}(\mathbf{X}, \mathbf{X}_*). \end{aligned} \quad (5)$$

Given a novel input in the test data set, the above posterior mean gives the prediction, while the posterior covariance gives the uncertainty region of the prediction.

Kernel function determines the power of the GP model to a large extent. In order to make a kernel function full of expressive power and automatically adaptive to the data, the following work can be adopted. In [25], a spectral mixture (SM) kernel was proposed to approximate the spectral density with a Gaussian mixture model arbitrarily well in the frequency domain and transform it back into a universal stationary kernel. In [26], the authors modified the SM kernel to be a linear multiple low-rank sub-kernels with a favorable difference-of-convex optimization structure. In [27], DNN architecture was combined with automatic relevance determination (ARD) kernel to approximate any kernel function (including both the stationary and non-stationary ones). Yet a fresher way of designing universal kernel is through designing deep GP models [28] and through linking DNN to GP [29, 30], which remains a promising while challenging research direction.

Next, we introduce the classical ML-based GP hyper-parameter estimation. Due to the Gaussian assumption on the noise, the log-likelihood function can be obtained in closed form. The GP hyper-parameters can be tuned equivalently by minimizing the negative log-likelihood function (after ignoring the unrelated terms) as

$$l(\mathbf{X}, \mathbf{y}; \theta) = \mathbf{y}^T \mathbf{C}^{-1}(\theta) \mathbf{y} + \log \det(\mathbf{C}(\theta)), \quad (6)$$

where $\mathbf{C}(\theta) \triangleq \mathbf{K}(\mathbf{X}, \mathbf{X}; \theta_h) + \sigma_e^2 \mathbf{I}_n$. This optimization problem is mostly solved via gradient based methods, such as

LFGS-Newton or conjugate gradient [1], which requires the following partial derivatives for $i = 1, 2, \dots, p$ in closed form:

$$\frac{\partial l(\theta)}{\partial \theta_i} = \text{tr} \left(\mathbf{C}^{-1}(\theta) \frac{\partial \mathbf{C}(\theta)}{\partial \theta_i} \right) - \mathbf{y}^T \mathbf{C}^{-1}(\theta) \frac{\partial \mathbf{C}(\theta)}{\partial \theta_i} \mathbf{C}^{-1}(\theta) \mathbf{y}.$$

It is noted that minimizing the negative log-likelihood in Eq.(6) with respect to θ may easily lead to a bad local optimum when a learning model is over-parameterized and the cost function is non-convex in terms of θ without any favorable optimization structure.

3.3. DNN Versus GP

In the previous subsections, we briefly introduced DNN and GP that can both be used as the core learning module of the FedLoc. DNN is quite popular nowadays due to various good reasons. Among others, it can approximate any smooth function according to the universal approximation theorem [22]. But the main drawbacks of DNN lie in its inadequate interpretability and the large number of hyper-parameters (DNN weights) to be trained. For our FedLoc framework proposed in this paper, we put more emphasis on GP due to their unique welcome features as compared with DNN.

First, GP involves significantly fewer model hyper-parameters than an equally-effective DNN. From [31] we know that a single layer Bayesian neural network with i.i.d. weights converges to a GP. Correspondingly, a neural network kernel was designed with the following explicit form [1]:

$$k_{NN}(\mathbf{x}, \mathbf{x}') = \frac{2}{\pi} \sin^{-1} \left(\frac{2\tilde{\mathbf{x}}\Sigma\tilde{\mathbf{x}'}}{\sqrt{(1+2\tilde{\mathbf{x}}\Sigma\tilde{\mathbf{x}})(1+2\tilde{\mathbf{x}}'\Sigma\tilde{\mathbf{x}'})}} \right), \quad (7)$$

where $\tilde{\mathbf{x}} \triangleq [1, \mathbf{x}^T]^T$ is an augmented input vector. Often, we assume $\Sigma = \text{diag}(\sigma_1^2, \sigma_2^2, \dots, \sigma_{d+1}^2)$ to be a diagonal matrix, thus the hyper-parameters $\theta_h = [\sigma_1^2, \sigma_2^2, \dots, \sigma_{d+1}^2]^T$ is of dimension $d+1$. If Σ is taken to be a general matrix, the hyper-parameters to be tuned is in the order of d^2 , being much smaller than the size of a fully-connected DNN in most cases.

Lately, the arc-cosine kernels [32], the neural tangent kernel (NTK) [33], and the convolutional neural tangent kernel (CNTK) [34] were developed to mimic DNN. The hyper-parameter is only the number of layers that can be tuned easily using cross-validation. Performance wise, the NTK is able to capture the behavior of fully-connected DNN with infinite width, which is impossible to be trained otherwise using back-propagation and gradient descent type optimization methods. More and more deep kernels will be proposed in the future as we get better understanding on the connections between DNN and GP [29, 30]. In our application, we aim to train a global model that is capable of representing the large amount of data collected by massive number of collaborating mobile users, for which a sophisticated, large model is highly demanded. A recent study in [35] claims that a DNN can improve the training and test performance continuously when the size of the model

increases beyond a threshold. Lastly, we must note that there are also various interesting concurrent works on reducing the size of a fully-connected neural network, for instance, using model distillation [36] and model sparsification [37].

Second, GP model can handle input uncertainty naturally. For our application, the model inputs often involve position or position related measures that are intrinsically subject to noise due to the imperfect field calibration. Since GP model is a probabilistic model, the input uncertainty can be easily handled. We could assume the training input \mathbf{x} to be a random variable with known distribution $p(\mathbf{x})$. According to [38], the mean function of GP with input uncertainty can be obtained via:

$$\tilde{m}(\mathbf{x}) = \int m(\mathbf{x})p(\mathbf{x})d\mathbf{x}, \quad (8)$$

and the kernel function can be obtained via:

$$\tilde{k}(\mathbf{x}, \mathbf{x}') = \iint k(\mathbf{x}, \mathbf{x}')p(\mathbf{x})p(\mathbf{x}')d\mathbf{x}d\mathbf{x}'. \quad (9)$$

The only difficulty lies in the evaluation of the two integrals. In general, the two integrals can be solved by sampling methods [39]. The rest of the steps remain the same as the standard GP with clean input as given in (1). The computation can be largely reduced for Gaussian distribution of the input \mathbf{x} using unscented transform, see for instance [40, Chapter 5.5]. Hence the computational complexity for both training and prediction increases only modestly as compared with that of the clean input case.

Third, GP model can encode prior information about the data more easily than the DNN. This inherits from the meaningful interpretation of various elementary kernels with known characteristics. For instance, when the data demonstrate periodicity, we could add elementary periodic kernel(s) or locally periodic kernel(s) to the eventual kernel; when the data demonstrate linear rising trend, we could add a linear kernel to the eventual kernel; when the data profile is known to be smooth, we could use the squared-exponential (SE) kernel with a large length scale parameter. Taking into account the prior information about the data can be regarded as regularizing the whole fitting process, thus is useful for avoiding data overfitting. This is a welcome feature for our applications in which the total amount of data is large but each mobile user may only have a small amount of local data in hand for training the global model.

Fourth, according to a recent white paper released by Huawei, wireless big data in 6G will essentially be produced as a consequence of small local data from huge amount of mobile users and IoT devices. When training with local data under the umbrella of federated learning, GP models coming from the Bayesian family are believed to be more advantageous owing to the fact that a well selected GP prior can work as a regularizer to avoid overfitting a sophisticated model with insufficiently small data.

Before we leave this section, it is noteworthy that the DNN and its variants are still more widely used than GP for machine

learning empowered applications. But for localization applications using the FedLoc framework, we believe GP models are more promising due to the aforementioned advantages.

4. FEDERATED LOCALIZATION (FEDLOC)

After having introduced the learning models as the main building blocks in Section 3, we can formally introduce the new proposed FedLoc framework in this section. In Subsection 4.1, the main idea of federated learning is introduced, followed by a review of various existing distributed training methods proposed for DNN and GP learning models in Subsection 4.2. For clarity, we also summarize the whole procedure of the FedLoc framework at the end of the section.

4.1. A Brief Review of Federated Learning

The idea of federated learning exists for a long time in the context of distributed learning and given the name by some researchers at Google in 2016 [41, 2]. Federated learning is a flexible but safe cooperation framework for mobile users. The idea behind federated learning is to approximate a global model/objective as a summation of local models/objectives trained individually by mobile users. Mathematically, the above idea can be expressed as

$$l(\mathbf{X}, \mathbf{y}; \boldsymbol{\theta}) \approx \sum_{k=1}^K l^{(k)}(\mathbf{X}_k, \mathbf{y}_k; \boldsymbol{\theta}), \quad (10)$$

where \mathbf{X} is the complete set of the training inputs, \mathbf{y} is the complete set of the training outputs, and they constitute the complete training set \mathcal{D} ; $l(\cdot)$ is a global objective that takes the complete training set and parameterized in the hyper-parameters $\boldsymbol{\theta}$; while \mathbf{X}_k is the k -th local set of the training inputs, \mathbf{y}_k is the k -th local set of the training outputs, and they constitute \mathcal{D}_k , which is a subset of \mathcal{D} ; $l^{(k)}(\cdot)$ is a local objective that only takes the k -th local data set, \mathcal{D}_k ; K is the total number of collaborating mobile users, which is assumed to be large. Both $l(\cdot)$ and $l^{(k)}(\cdot)$ are composite functions of a selected learning model and a cost. Lastly, we note that the outputs \mathbf{y} are mostly positions or position related measures in our work.

To shed some light on the objective $l(\cdot)$, let us consider the following two different machine learning models and their cost functions.

I: DNN with Least-Squares Cost. The global objective for training a DNN is given as follows:

$$l(\mathbf{X}, \mathbf{y}; \boldsymbol{\theta}) = \sum_{i=1}^n (y_i - f(\mathbf{x}_i; \boldsymbol{\theta}))^2, \quad (11)$$

where the outputs are assumed to be i.i.d. and $f(\mathbf{x}_i; \boldsymbol{\theta})$ is represented by a DNN with L hidden layers [24] with $\boldsymbol{\theta} = \{\mathbf{W}_0, \mathbf{W}_1, \mathbf{W}_2, \dots, \mathbf{W}_L\}$ representing the DNN weights to be tuned for all hidden layers. It is obvious that the global objective is already in the form of summation.

II: GP with Maximum Likelihood Cost. Due to the Gaussian assumption on the noise, the log-likelihood function can be obtained in closed form. Therefore, the global objective for training the GP regression model hyper-parameters is of the form

$$\begin{aligned} l(\mathbf{X}, \mathbf{y}; \boldsymbol{\theta}) &= \log p(\mathbf{y}; \mathbf{X}, \boldsymbol{\theta}) \\ &= \log \mathcal{N}(\mathbf{y}; \mathbf{m}(\mathbf{X}), K(\mathbf{X}, \mathbf{X}; \boldsymbol{\theta})), \end{aligned} \quad (12)$$

where the vector $\mathbf{m}(\mathbf{X})$ and the matrix $K(\mathbf{X}, \mathbf{X}; \boldsymbol{\theta})$ are respectively the mean function $m(\mathbf{x})$ and the kernel function $k(\mathbf{x}, \mathbf{x}'; \boldsymbol{\theta})$ evaluated for the complete data set \mathcal{D} . This global objective is not directly in the form of summation, but commonly approximated by the product-of-expert (PoE) [42] as

$$l(\mathbf{X}, \mathbf{y}; \boldsymbol{\theta}) \approx \sum_{i=1}^K \log \mathcal{N}(\mathbf{y}_k; \mathbf{m}(\mathbf{X}_k), K(\mathbf{X}_k, \mathbf{X}_k; \boldsymbol{\theta})). \quad (13)$$

Here, we note that the independent noise term has been absorbed into the kernel function for notation brevity in Eq.(13). In this paper, we will place more emphasis on GP models as they can provide natural uncertainty region of a prediction, which is vital for a basket of decision-critical applications.

4.2. Distributed Training of Learning Models

The original goal is to train a global model through

$$\hat{\boldsymbol{\theta}} = \arg \min_{\boldsymbol{\theta}} l(\mathbf{X}, \mathbf{y}; \boldsymbol{\theta}), \quad (14)$$

where the objective function is in general non-convex and often solved by gradient descent type methods as

$$\boldsymbol{\theta}^\eta = \boldsymbol{\theta}^{\eta-1} - \gamma \nabla_{\boldsymbol{\theta}} l(\mathbf{X}, \mathbf{y}; \boldsymbol{\theta}^{\eta-1}). \quad (15)$$

When the complete data set is large, the training of this global model will be computationally expensive. Federated learning aims to distribute the heavy computation load to a massive number of collaborating mobile users by considering the following problem:

$$\hat{\boldsymbol{\theta}} = \arg \min_{\boldsymbol{\theta}} \sum_{k=1}^K l^{(k)}(\mathbf{X}_k, \mathbf{y}_k; \boldsymbol{\theta}). \quad (16)$$

Each mobile user maintains a local update of the global model hyper-parameters and send it to the central node for consensus. There exist various ways for updating global model hyper-parameters. In the following, we focus on the classical federated averaging (FedAvg) [2] algorithm and algorithms developed upon alternating direction of multipliers method (ADMM) [43, 44].

Most straightforwardly, the k -th mobile user calculates the gradient $\nabla l^{(k)}(\boldsymbol{\theta})$ and upload it to the central node. The central node then aggregates a batch of/all gradients to approximate $\nabla_{\boldsymbol{\theta}} l(\mathbf{X}, \mathbf{y}; \boldsymbol{\theta})$. We illustrate the above workflow

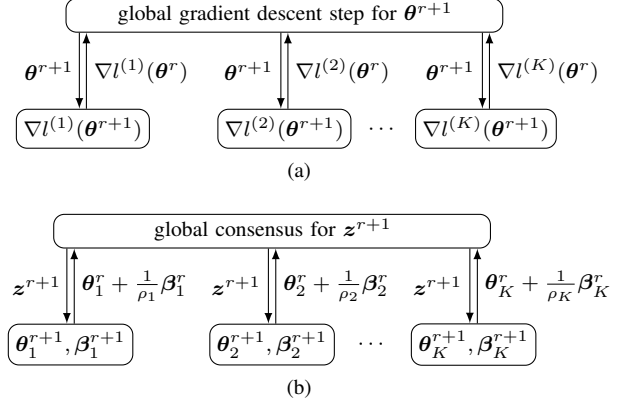


Fig. 3. Workflow of two existing distributed hyper-parameter optimization schemes. (a) FedAvg [2]. (b) cADMM [43].

in Fig. 3(a), and it is known as FedAvg and forms the optimization algorithmic core of the original federated learning framework [2]. More details about the FedAvg algorithm as well as its performance on several classical machine learning data sets can be found in [2]. A robust variation, called FedProx [45], can also be adopted to improve local training convergence by adding an extra proximal step at each client to restrict the distance between the local parameter estimates and the current global estimate.

Next, we will introduce two advanced ADMM optimization schemes, that can potentially balance the computation and communication efficiency. The first one, namely the classical ADMM based hyper-parameter optimization scheme (short as cADMM) reformulates the problem in (16) as a nonconvex consensus problem [43] with a set of newly introduced local hyperparameters $\{\boldsymbol{\theta}_1, \boldsymbol{\theta}_2, \dots, \boldsymbol{\theta}_K\}$ and the global hyperparameter \mathbf{z}

$$\begin{aligned} \min \quad & \sum_{k=1}^K l^{(k)}(\boldsymbol{\theta}_k), \\ \text{s.t.} \quad & \boldsymbol{\theta}_k - \mathbf{z} = \mathbf{0}, \quad \forall k = 1, 2, \dots, K, \end{aligned} \quad (17)$$

where $l^{(k)}(\boldsymbol{\theta}_k)$ is nonconvex in terms of the local hyperparameter $\boldsymbol{\theta}_k$ in general. The augmented Lagrangian function for (17) is given by

$$\begin{aligned} \mathcal{L}(\{\boldsymbol{\theta}_k\}, \mathbf{z}, \{\boldsymbol{\beta}_k\}) &= \sum_{k=1}^K (l^{(k)}(\boldsymbol{\theta}_k) + \boldsymbol{\beta}_k^T (\boldsymbol{\theta}_k - \mathbf{z})) \\ &\quad + (\rho_k/2) \|\boldsymbol{\theta}_k - \mathbf{z}\|_2^2, \end{aligned} \quad (18)$$

where $\boldsymbol{\beta}_k$ is the dual variable and ρ_k stands for a predetermined regularization parameter. The $(r+1)$ -th iteration of cADMM for solving (17) could be decomposed as:

$$\mathbf{z}^{r+1} = (1/K) \sum_{k=1}^K (\boldsymbol{\theta}_k^r + (1/\rho_k) \boldsymbol{\beta}_k^r), \quad (19a)$$

$$\begin{aligned} \boldsymbol{\theta}_k^{r+1} &= \arg \min_{\boldsymbol{\theta}_k} (l^{(k)}(\boldsymbol{\theta}_k) + (\boldsymbol{\beta}_k^r)^T (\boldsymbol{\theta}_k - \mathbf{z}^{r+1}) \\ &\quad + (\rho_k/2) \|\boldsymbol{\theta}_k - \mathbf{z}^{r+1}\|_2^2), \end{aligned} \quad (19b)$$

$$\boldsymbol{\beta}_k^{r+1} = \boldsymbol{\beta}_k^r + \rho_k (\boldsymbol{\theta}_k^{r+1} - \mathbf{z}^{r+1}). \quad (19c)$$

The above workflow is shown in Fig. 3(b).

Next, we continue to introduce a more recent proximal ADMM (short as pxADMM) scheme proposed in [44], which is capable of reducing the communication overhead and computational time *at the same time*. Unlike in step (19b) where local hyperparameters θ_k are updated by minimizing the augmented Lagrangian function exactly, the proximal ADMM takes a proximal step w.r.t. θ_k by applying first-order Taylor expansion to $l^{(k)}(\theta_k)$ [44], i.e.,

$$\begin{aligned} \theta_k^{r+1} = \arg \min_{\theta_k} \nabla^T l^{(k)}(z^{r+1})(\theta_k - z^{r+1}) \\ + (\beta_k^r)^T (\theta_k - z^{r+1}) + \left(\frac{\rho_k + L_k}{2} \right) \|\theta_k - z^{r+1}\|_2^2, \end{aligned} \quad (20)$$

where L_k is a positive constant for $\|\nabla l^{(k)}(\theta_k) - \nabla l^{(k)}(\theta'_k)\| \leq L_k \|\theta_k - \theta'_k\|$ to be satisfied for all θ_k and θ'_k , $k = 1, 2, \dots, K$. Note that the proximal step (20) for θ_k is a (convex) quadratic optimization problem leading to the following closed-form solution:

$$\theta_k^{r+1} = z^{r+1} - \left(\frac{(\nabla l^{(k)}(z^{r+1}) + \beta_k^r)}{\rho_k + L_k} \right). \quad (21)$$

The $(r+1)$ -th iteration of the pxADMM for solving (17) is decomposed as:

$$z^{r+1} = (1/K) \sum_{k=1}^K (\theta_k^r + \frac{1}{\rho_k} \beta_k^r), \quad (22a)$$

$$\theta_k^{r+1} = z^{r+1} - \frac{(\nabla l^{(k)}(z^{r+1}) + \beta_k^r)}{\rho_k + L_k}, \quad (22b)$$

$$\beta_k^{r+1} = \beta_k^r + \rho_k (\theta_k^{r+1} - z^{r+1}). \quad (22c)$$

The pxADMM shares the same workflow with the cADMM as depicted in Fig. 3(b). Criteria for choosing ρ_k and L_k are given in [44], where the authors also proved under mild conditions that 1) for all k , θ_k^r converge to z^r ; and 2) $(\{\theta_k^r\}, z^r, \{\beta_k^r\})$ converges to a stationary point of (17).

It is easy to see that the pxADMM reduces the communication overhead in the same way as cADMM does. However, the proximal step shown in (22b) leads to an inexact, but closed-form solution of the local sub-problem (19b) with rather cheap computation cost. Although more iterations may be required towards convergence, the overall computational time can be well reduced.

Federated learning emphasizes strongly on the mobile user's sole ownership of data and protection of data privacy. Privacy preservation in federated learning can be achieved by various security techniques like secure multi-party computation, homomorphic encryption and differential privacy. Message encryption is beyond the scope of this paper, and interested readers can refer to [46]. Here, we note that no matter which distributed model training method (FedAvg or cADMM or pxADMM) is adopted, the mobile users do not need to report the raw data that contain location information and other privacy related information to be strictly protected. Unlike for images with strong local correlation in pixels, there is no evidence about recovering a user's raw data from local gradients or hyper-parameter estimates intercepted by malicious users.

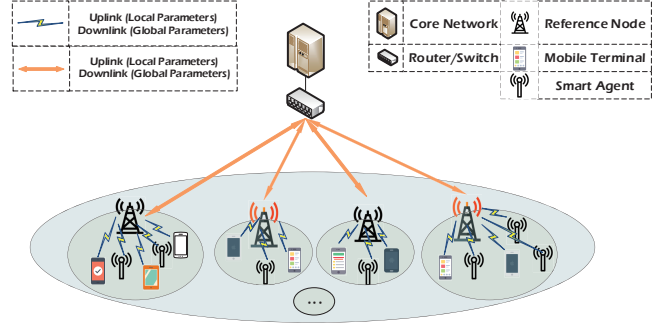


Fig. 4. A network infrastructure that supports the proposed FedLoc framework. For illustration purposes, the whole deployment area is divided into many non-overlapping sub-areas, and for each sub-area there is a mobile terminal collecting data. Each terminal can travel the whole deployment area for collecting data.

5. NETWORK INFRASTRUCTURE FOR FEDLOC

The FedLoc framework may need to communicate a big number of model parameters repeatedly over the air, especially when DNN is adopted as the learning model. In this section, we introduce two practical network infrastructures to meet the communication requirement of the proposed FedLoc framework.

5.1. Cloud-based Infrastructure

For ease of understanding, a complete picture of the network infrastructure is depicted in Fig. 4 for cooperative localization purposes. The key elements of this network as well as their functionality are summarized as follows:

1. *Reference Network Node*, equipped with cache, storage, and communication entities. A reference network node communicates with the mobile terminals deployed in its communication range to exchange learning model related information. Both the position and the transmit power of a reference network node are assumed to be precisely known. Representative reference network nodes include 5G macro and micro base stations, Wi-Fi access points, BLE beacons, etc. Especially the new 5G and Wi-Fi network are able to provide low-latency, high throughput wireless transmission to FedLoc which requires to transmit a big amount of model parameters in every iteration. Table 1 gives more details. For better intuitions, two specific examples are given below. The 5G network with the highest throughput can support a 9-layer fully-connected DNN with the network layout “20000-30000-10000-100000-10000-10000-10000-1000-10” that has around 300 million weights. The 4G network, however, can

Wireless infrastructure	Max uplink data rate (Mbps)	Max downlink data rate (Mbps)	Number of DNN weights (Million)	Configuration
5G [47]	10,000	20,000	312.5	IMT-2020 peak rate
4G [48]	500	1000	15.625	IMT-advanced
WiFi-6(ax) [49]	2400	2400	75	160MHz 2*2MIMO 1024-QAM 802.11ax
WiFi-5(ac) [50]	1733	1733	54.16	160MHz 2*2MIMO 256-QAM 802.11ac

Table 1. Downlink and uplink data rate of different wireless infrastructures and the the number of parameters (taking the weights of DNN as an example) that can be supported. The number of the DNN weights (in million) shown in the fourth column was computed by dividing the uplink rate (given in the second column) by 32 bits per DNN weight.

only support a 8-layer fully-connected DNN with a much smaller network layout “5000-5000-10000-3000-9000-2000-200-10” with around 15 million weights.

2. *Mobile Terminal (MT)*, equipped with sensing, logging, computing, storage, and communication entities. Moreover, the MT has designated mobile applications installed already for the calibration work. The MT collects position related measurements, trains a local update of the global learning model parameters, and uploads them to the core network. All the computations are conducted on-device using only the local data. Here, the mobile terminal refers to a smartphone specifically. It is noteworthy that modern smartphones are equipped with a basket of inertial sensors, including accelerometer, gyroscope, magnetometer, barometer, pedometer, barcode/QR code sensors, that can be exploited for localization or localization-related tasks.

Apart from the rapid development of the hardware, a number of mobile machine learning platforms are under development, such as Tensorflow by Google, Core ML by Apple, Caffe2 by Facebook, Paddle Lite by Baidu, MNN by Alibaba, etc. Mobile users can easily deploy different deep learning models on their smartphones in the near future.

3. *Core Network*, equipped with high speed computing, cache/storage and communication entity. The local updates from the mobile users are aggregated to the core network to compute a global parameter update. When the training phase is over, the resulting global learning model will be stored in the core network and used for predicting a new position. Since the heavy computations have been allocated to mobile users, the core network can focus on smarter coordination of different tasks and resources, so as to make the whole network agile and adaptive to changing environments.
4. *Fixed Smart Agents*, equipped with sensing, logging, computing, storage and communication entities. Such smart agents include IoT machines, smart traffic light,

micro-base stations in 5G that are collecting location data. Unless these smart agents belong to different operators, the collected data are often not subject to privacy matters.

For clarity, we give a complete procedure of the federated wireless localization framework in Algorithm 1, which works both for cooperative localization and cooperative location data processing.

5.2. Edge-based Infrastructure

In the second infrastructure, the mobile users or smart agents can upload their local data to a trustful third-party edge node, where there is sufficient storage and computation power. This third-party edge node first pre-processes the received data and distributes it to a number of computing units for processing. Each edge node is in charge of building a locally-global learning model and transmits the key parameters to the core network for central control. This infrastructure is more suitable for building a number of regional global models for location data processing. The third use case that we will show in the next section can potentially benefit this infrastructure. For clarity, we show this alternative network infrastructure in Fig.5. Accordingly, Algorithm 1 can be slightly revised to accommodate this network infrastructure.

6. USE CASES OF FEDLOC

To better understand the work mechanism of the FedLoc framework, we will introduce various use cases of the FedLoc framework in this section. To be precise, we consider: (1) DNN based static localization/finger printing; (2) DNN based smartphone sensor calibration for accurate navigation with low-sampling-rate GPS; (3) GP based state-space model for target tracking and navigation; and (4) GP based wireless traffic prediction in 5G C-RAN. The first three use cases are for localization, while the last one is for location data processing and prediction. Most of the above uses cases were summarized from our recent applications.

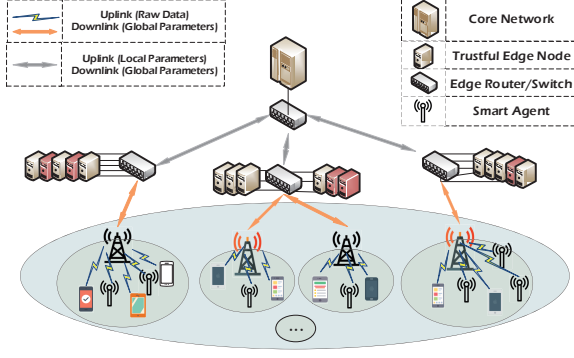


Fig. 5. An alternative network infrastructure for the FedLoc framework that uses edge nodes.

6.1. DNN-Based Static Localization

For static localization, there exist various statistical methods using wireless measurements, such as ToA, RSS, proximity [51, 52]. These methods mostly rely on empirical propagation models. In this subsection, we show a different static localization method using DNN, which can benefit from the federated learning framework. DNN based localization is preferred for complicated wireless environments, for which the empirical models are difficult to capture the underlying propagation mechanism, possibly also changing over time.

Let us take a look at three representative indoor scenarios:

- **Indoor shopping mall**, where there are a bunch of WiFi/BLE access points and micro base stations for public data traffic. In addition, thanks to the rapid spread of 5G for internet-of-things (IoT) and machine type communications (MTC), there are now a big number of machines/landmarks with QR codes in the shops. By scanning the QR codes, a customer can easily get shopping mall information, promotion information and make transactions. Some live examples are demonstrated in Fig. 6.
- **Indoor museum**, where there are a bunch of WiFi/BLE access points in the exhibition rooms and a considerable number of QR labels beside the exhibits to serve as references. Similarly, by scanning the QR codes a visitor can easily obtain detailed interpretation of the exhibits on his/her mobile terminal. Some live examples are demonstrated in Fig. 7.
- **Indoor office**, where there are a bunch of WiFi/BLE access points in the whole office area and a huge number of QR labels placed at the entrance of each meeting room, on all valuable assets, such as computers, tables, coffee machines, etc.

The DNN based localization method that we introduce here needs to be trained using a big data set \mathcal{D} , where the training

Algorithm 1: FedLoc Framework

Input: A massive collaborating mobile terminals with index $k = 1, 2, \dots, K$; Local data $\mathcal{D}_k = \{\mathbf{X}_k, \mathbf{y}_k\}$, where the inputs and outputs are positions/position related measures, depending on the applicationA learning model, for instance a DNN or a GP model.

Output: Optimal hyper-parameters θ^* of the global learning model for localization.

- 1 **Initialization:** Initial hyper-parameters of the selected learning model, θ^0 ; iteration index, $\eta = 0$.
- 2 **for** (outer iterations) $\eta = 0, 1, \dots$ **do**
- 3 1. The core network sends a probing signal to all the mobile terminals and identify which are idle during this round. The idle terminals form a set, \mathcal{K}_η .
- 4 2. The core network sends a seed to the selected terminals for encoding the messages as well as the current hyper-parameter estimate, θ^η .
- 5 **for** (inner iterations) each idle mobile terminal $k \in \mathcal{K}_\eta$ in parallel **do**
- 6 1. Use the full local data, \mathcal{D}_k , or a fraction of it to update the hyper-parameter as $\theta_k^{\eta+1}$, for instance, via FedAve or FedProx for DNN models or via ADMM or proximal ADMM for GP models.
- 7 2. Encrypt the local update of the global model hyper-parameters as a message.
- 8 3. Send the encrypted message first via wireless link to the nearest reference node and routed then to the core network, supported by the first network infrastructure.
- 9 **end**
- 10 3. The core network receive all the encrypted messages from the mobile terminals in \mathcal{K}_η and perform decryption.
- 11 4. The core network updates the global learning model hyper-parameter via consensus.
- 12 5. Finish this round and reset $\eta = \eta + 1$.
- 13 6. Repeat the above iterations until certain stopping criteria are satisfied.
- 14 **end**
- 15 The final optimal hyper-parameters is $\theta^* = \theta^\eta$.

input, \mathbf{X} , contains the radio features at different locations and the training output, \mathbf{y} contains the corresponding locations. As a concrete example, we assume that a training input comprises RSS obtained with respect to P WiFi/BLE access points, $\mathbf{x}_i = [RSS_{i,1}, RSS_{i,2}, \dots, RSS_{i,P}]$ and the output \mathbf{y} is a position (2D or 3D) at which the radio feature is measured. Note that an output \mathbf{y}_i is either measured precisely at the calibration points by paid workers or imprecisely (for instance, with the aid of the landmark points and manual click on the indoor map displayed on the mobile application) by voluntary users.



Fig. 6. All the QR labels were photoed in a modern shopping mall in Shenzhen, China. (a) QR codes to be scanned for ordering foods and paying the bill for a specific table in the restaurant; (b) QR code to be scanned for promotion information at a shop; (c) QR codes for various different services, including product recommendation, payment, etc at the cashier of a shop; (d) QR code on a vending machine for borrowing and returning mobile power bank, moreover, the vending machine can be seen as a landmark as well.



Fig. 7. Exhibits with QR codes photoed at the Palace museum in Beijing.

In either case, we assume the output is subject to additional independent noise. A concrete example is illustrated in Fig. 8. Various works on using DNN and RSS measurements for indoor fingerprinting have been published in recent years, for instance [53, 54], but they are in form of centralized algorithms and can be implemented in a distributed manner using our FedLoc framework.

The regression problem is thus formulated as:

$$\mathbf{y}_i = f(\mathbf{x}_i; \boldsymbol{\theta}) + \mathbf{n}_i, \quad (23)$$

where $f(\mathbf{x}_i; \boldsymbol{\theta}) : \mathbb{R}^{dx} \rightarrow \mathbb{R}^{dy}$ represents a DNN with an input of $dx = P$ features, \mathbf{x}_i , and the neural network weights, $\boldsymbol{\theta}$, to be tuned; and \mathbf{n}_i represents the noise. The function $f(\mathbf{x}_i; \boldsymbol{\theta})$ is also known as RSS map or fingerprinting map in some other contexts.

In order to adopt the federated learning framework, we deploy a big number of mobile terminals, each is responsible for a

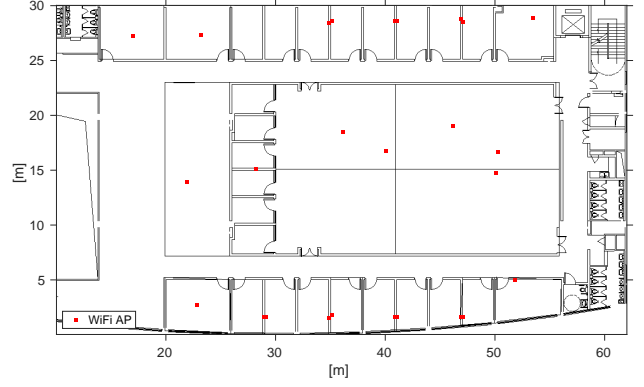


Fig. 8. A typical indoor office environment at the Chinese University of Hong Kong (Shenzhen), where two dozens of WiFi access points are deployed in offices and laboratories. For this conceptual example, an input, \mathbf{x}_i , is a vector of $P = 26$ RSS values, and the corresponding output, $\mathbf{y}_i = [p_i^x, p_i^y]$ is a 2D position.

particular area, possibly overlapping with its neighboring areas. The k -th mobile terminal collects a data set $\mathcal{D}_k = \{\mathbf{X}_k, \mathbf{y}_k\}$ and use it to train a local update of the global parameters. For simplicity, we assume that all mobile users have the same data structure. Then, each mobile user solves

$$\boldsymbol{\theta}_k = \arg \min_{\boldsymbol{\theta}} \sum_{\forall \{\mathbf{x}_i, \mathbf{y}_i\} \in \mathcal{D}_k} \|\mathbf{y}_i - f(\mathbf{x}_i; \boldsymbol{\theta})\|_2^2. \quad (24)$$

All the mobile terminals cooperate to perform Algorithm 1. Since in this use case, the global objective is readily in the form of summation, we can set the weights β_k to be the ratio $|\mathcal{D}_k| / \sum_{j \in \mathcal{K}_\eta} |\mathcal{D}_j|$ in the η -th iteration and update $\boldsymbol{\theta}^{\eta+1} = \sum_{k \in \mathcal{K}_\eta} \beta_k \boldsymbol{\theta}_k^\eta$. When the messages are exchanged between the core network and mobile terminals, they are first encrypted in the mobile terminals and decrypted in the core network. The workflow of the FedLoc for DNN based static localization is shown in Fig. 9.

When the training terminates, the central node will obtain a global model with the optimized hyper-parameter estimate, denoted by $\hat{\boldsymbol{\theta}}$. Given a new vector of RSS measurements, $\mathbf{x}_* = [RSS_{*,1}, RSS_{*,2}, \dots, RSS_{*,P}]$ reported by a to-be-located mobile user to the central node, the trained learning model will map it to the output, namely the desired position estimate, through $\mathbf{p}_* = f(\mathbf{x}_*; \hat{\boldsymbol{\theta}})$.

A final remark of this subsection is the following. When using a deep learning model in the federated wireless localization framework, the final position estimate, \mathbf{p}_* , is merely a point estimate without any information about its reliability. The fusion of the local estimates, point estimates as well, might be disastrous due to the notorious black-box nature and overfitting phenomena of DNN. Alternatively, replacing the canonical deep learning model with a (Bayesian) GP model or a Bayesian neural network (BNN), one can instead obtain a

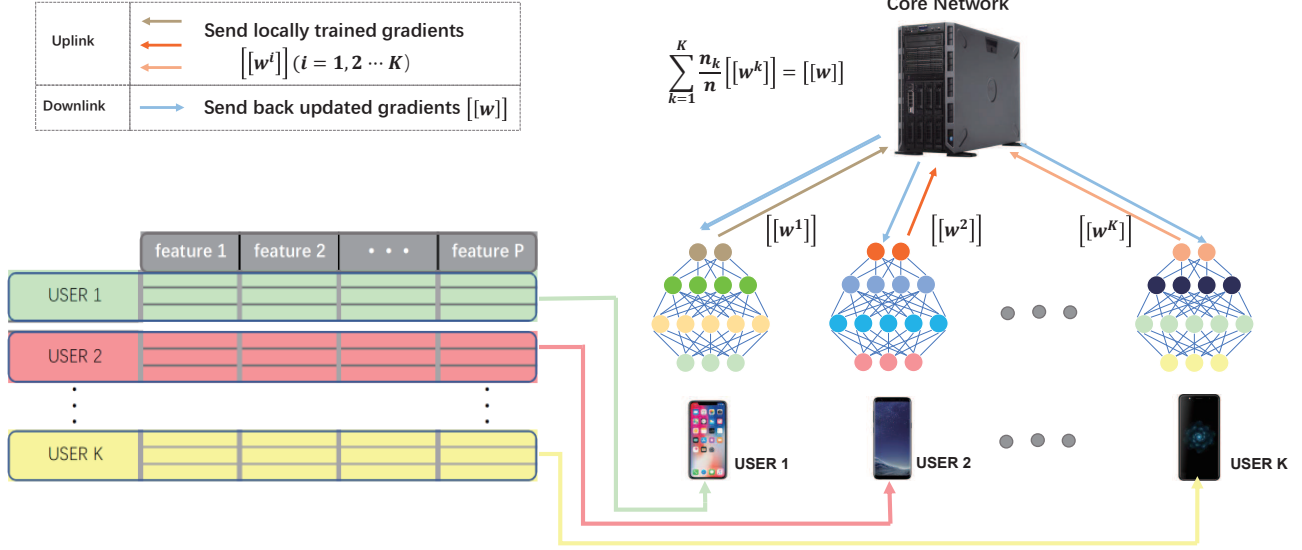


Fig. 9. Illustration of DNN based static localization. Here, $[[W]]$ represents encrypted NN weight parameters using for instance Homomorphic Encryption (HE).

posterior distribution of the desired position, $p(p_*|\mathcal{D})$, from which a point estimate as well as a natural uncertainty region of this estimate can be easily derived.

6.2. DNN-Based Vehicle Navigation with Low Sampling Rate GPS

For land vehicle navigation, combining inertial measurement unit (IMU) and global positioning system (GPS) embedded in a smartphone is still the main-stream technical solution. The GPS can readily provide accurate vehicle positions when the majority of the satellite signals are in line-of-sight (LOS) propagation with relatively high received signal strength. The IMU comprises, primarily, a three-axis acceleration sensor and a three-axis gyroscope to determine both the position and the velocity of a vehicle. The main functionality of the IMU is to provide vehicle positions with much higher sampling rate (> 50 Hz) between two consequent GPS positions (normally sampled with 1 Hz). Unfortunately, when a vehicle enters into areas with severe signal blockage, the received GPS signals will be very weak or even undetectable thus lead to significantly degraded position estimates as compared with the LOS case. Solely using low-end IMU measurements for high-accuracy navigation is demanded but still immature due to the sensor biases, scale-factor errors, and other random errors accumulated over the time. When strong GPS signals are constantly available, the IMU measurements can be well calibrated to alleviate the sensor error aggregation problem. But how can we maintain a similar positioning accuracy level for the case that only a few GPS signals are available occasionally for harsh wireless environments, such as city center and forest?

Undoubtedly, we hope the solution is easy to implement on smartphones with affordable computational complexity.

Towards this end, we introduce in this subsection a machine learning-based approach that can be implemented on commercial smart phones with low-end inertial sensors and GPS for vehicle navigation, and is able to maintain good navigation accuracy but using low-sampling-rate GPS signals. Inertial sensors are used to continuously estimate the vehicle velocity and position at a high sampling rate as the backbone and the low-sampling-rate GPS signals are used for IMU calibration every once a while (for example every 60 seconds). When the GPS signals are not available, we use two trained DNNs to calibrate/adjust the inertial sensor readings; when a high-quality GPS signal arrives, we use it to reset the inertial sensor readings. In this way, we aim to reduce the use of GPS signals.

In our machine learning-based approach, we adopt two DNNs to estimate/predict the velocity $v_{t,NN1}$ and the yaw angle $y_{t,NN2}$ of the vehicle, respectively. In the model training phase, both DNNs take the measurements of the smart phone inertial sensors as the input while the GPS velocity and yaw angle measurements are taken as the outputs/labels.

Concretely, the first DNN takes the following inputs:

- The velocity $\tilde{v}_t^n = ((v_t^{nx})^2 + (v_t^{ny})^2 + (v_t^{nz})^2)^{1/2}$ calculated from the inertial sensor data;
- The sequence of angular velocity $\{\omega_{t-l}^{bz}, \dots, \omega_t^{bz}\}$ of the vehicle;
- The sequence of smoothed linear acceleration along the front direction of the vehicle, denoted as $\{a_{t-l}^{nx}, \dots, a_t^{nx}\}$.

The DNN outputs the velocity $v_{t,NN1}$ benchmarked/labeled by the GPS velocity $v_{t,GPS}$. Similarly, the second DNN takes the following inputs:

- The sequence of smoothed linear acceleration, denoted as smooth $\{a_{by}, \dots, a_{by}\}$;
- The sequence of angular velocity $\{\omega_{t-l}^{bz}, \dots, \omega_t^{bz}\}$;
- The compensated yaw sequence $\{y_{t-l}, \dots, y_t\}$.

The DNN outputs the yaw angle $y_{t,NN2}$ benchmarked/labeled by the GPS yaw angle $y_{t,GPS}$. Our previous work presented a centralized framework in [55], where interested readers can find great details about the measurements, configurations of the DNNs, as well as a diagram of the whole navigation system. In this paper, we are more keen on a federated learning empowered framework that benefits from collaborating mobile users when collecting training data over the whole deployment area. To this end, we let the two DNNs be trained individually by a batch of collaborating mobile users according to Algorithm 1 with the DNN weights optimized via the FedAve or the FedProx. The information exchange procedure remains the same as the one discussed in the previous subsection for static localization. In the online use phase, the two DNNs will calibrate the inertial sensor error aggregation when there is no GPS signal at hand.

6.3. GP-Based State-Space Model (GPSSM) for Target Tracking

State-space models are outstanding for modeling a time series $\mathbf{y}_{1:T} \triangleq \{\mathbf{y}_t\}_{t=1}^T$ with latent states $\mathbf{x}_{0:T} \triangleq \{\mathbf{x}_t\}_{t=0}^T$. An SSM is defined by a transition function, $f : \mathbb{R}^{dx} \rightarrow \mathbb{R}^{dx}$ and a measurement function, $g : \mathbb{R}^{dx} \rightarrow \mathbb{R}^{dy}$, commonly written as:

$$\begin{aligned} \mathbf{x}_t &= f(\mathbf{x}_{t-1}) + \mathbf{e}_{t-1}, \\ \mathbf{y}_t &= g(\mathbf{x}_t) + \mathbf{n}_t, \end{aligned} \quad (25)$$

where $\mathbf{x}_t \in \mathbb{R}^{dx}$ is the latent state, $\mathbf{y}_t \in \mathbb{R}^{dy}$ is the measurement, \mathbf{e}_t and \mathbf{n}_t are the process noise and measurement noise at time instance t , respectively. Traditional SSM restricts f and g to empirical parametric functions [10], whose parameters can be learned through expectation-maximization (EM) [56] or Markov chain Monte Carlo (MCMC) [57].

Since GP models provide outstanding performance in function approximation with a natural uncertainty bound, they have been adopted to model complicated nonlinear functions in the SSMs, leading to the elegant and promising GPSSM [58].

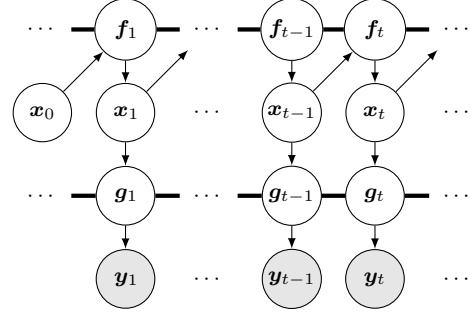


Fig. 10. Graphical representation of GPSSM. The shaded nodes denote measurements while the transparent nodes denote latent variables. Variables belonging to the same GP are connected by a thick edge.

A general GPSSM is given by

$$\begin{aligned} f(\mathbf{x}) &\sim \mathcal{GP}(m_f(\mathbf{x}), k_f(\mathbf{x}, \mathbf{x}'; \boldsymbol{\theta}_f)), \\ g(\mathbf{x}) &\sim \mathcal{GP}(m_g(\mathbf{x}), k_g(\mathbf{x}, \mathbf{x}'; \boldsymbol{\theta}_g)), \\ \mathbf{x}_0 &\sim p(\mathbf{x}_0), \\ f_t &= f(\mathbf{x}_{t-1}), \\ \mathbf{x}_t | f_t &\sim \mathcal{N}(\mathbf{x}_t | f_t, \mathbf{Q}), \\ g_t &= g(\mathbf{x}_t), \\ \mathbf{y}_t | g_t &\sim \mathcal{N}(\mathbf{y}_t | g_t, \mathbf{R}), \end{aligned} \quad (26)$$

with the model hyperparameters $\{\boldsymbol{\theta}_f, \boldsymbol{\theta}_g, \mathbf{Q}, \mathbf{R}\}$, where $\boldsymbol{\theta}_f$ and $\boldsymbol{\theta}_g$ are the kernel hyper-parameters of the GPs, \mathbf{Q} and \mathbf{R} are the covariance matrices of the process noise and the measurement noise, respectively. For clarity, Fig. 10 shows the graphical representation of a GPSSM. In the following, we will first introduce a naive GPSSM, which requires a big set of calibrated data to train the dynamic function f and the measurement function g , respectively. Later on, we will briefly mention an advanced variational GPSSM proposed in [58].

We start with the transition function in the naive GPSSM. The GP regression model for the transition function, f , is $\mathbf{x}_{t+1} = f(\mathbf{x}_t) + \mathbf{e}_t$, where the output $\mathbf{x}_{t+1} \in \mathbb{R}^{dx}$ is the state at time $t+1$; the unknown function $f(\mathbf{x}_t) : \mathbb{R}^{dx} \rightarrow \mathbb{R}^{dx}$ is essentially a multi-output GP [1]; and \mathbf{e} is a vector of noise terms. For ease of understanding, each entry of the state, say the j -th, is modeled as an independent GP as $[\mathbf{x}_{t+1}]_j = f_j(\mathbf{x}_t) + e$, where $f_j(\mathbf{x}_t) : \mathbb{R}^{dx} \rightarrow \mathbb{R}$ is a single-output GP. For this GP, we need to select a kernel function, $k_f(\mathbf{x}_t, \mathbf{x}_t'; \boldsymbol{\theta})$, that well represents the underlying correlations between the states at different time instances. The SE kernel and the ARD kernel are default kernels. Given a training data set of calibrated trajectories, $\mathcal{D}_j \triangleq \{\mathbf{X}, \hat{\mathbf{x}}_j\}$, where $\hat{\mathbf{x}}_j = [[\mathbf{x}_1]_j, [\mathbf{x}_2]_j, \dots, [\mathbf{x}_T]_j]^T$ is the vector comprising the outputs and $\mathbf{X} = [\mathbf{x}_0, \mathbf{x}_1, \dots, \mathbf{x}_{T-1}]^T$ is the matrix of all input vectors. In order to model the transition function using GP, both the input and the output are states but with a time lag. To train the GP hyper-parameters in a global batch manner, one could follow (12) and solve

for the ML hyper-parameter estimate. To be able to use the federated learning framework, one may use the approximation form given in (13) and let K mobile terminals collaborate to update the global ML hyper-parameter estimate with local data, namely the trajectories walked by each individual. When the training phase ends, the central node will obtain a global model with the optimized hyper-parameter estimate, denoted by $\hat{\theta}$. Given a new state, \mathbf{x}_* , the GP model will give a posterior distribution of the next state, $p([\mathbf{x}_*]_j | \mathcal{D}_j)$, which is also Gaussian. More details about this posterior inference step can be found in Section 2 of [1].

The GP regression model for the measurement function, g , is $\mathbf{y}_t = g(\mathbf{x}_t) + \mathbf{n}_t$, where the input $\mathbf{x}_t \in \mathbb{R}^{dx}$ is the state at time t , the output \mathbf{y}_t is a vector of state related wireless measurements, and the unknown function $f(\mathbf{x}_t) : \mathbb{R}^{dx} \rightarrow \mathbb{R}^{dx}$ is essentially another multi-output GP. Similar to the transition function case, we model an individual GP for each single entry of the output. The training of the measurement function, g , using GP models is similar to that of the training function, f , introduced above. Interested readers can find more details about the use of GPs for modeling f and g in [59, 60]. When both the transition and measurement GP models have been built, and the posterior distributions derived, they can be combined with the famous particle filter or smoother to reconstruct unknown trajectories. In [61], we proposed the first real indoor navigation prototype based on the GPSSM and achieved well improved navigation accuracy in various tests with real smartphone sensory data. Besides, we derived in [62] the posterior and parametric Cramer-Rao bound for filtering based on GPSSM.

In the GPSSM, the training of both GP models requires a data set with rather precise knowledge of the latent states. In a more advanced formulation [58, 63], variational inference techniques [64] is combined with the GPSSM so that the training of the GPSSM model hyper-parameters can be estimated jointly with the latent states. The variational GPSSM looks very elegant and does not require calibrated data, but at the expense of having to deal with a large scale optimization problem. In order to use the federated learning framework, one could combine the distributed variational technique [65] with the GPSSM.

6.4. GP-Based Wireless Traffic Modeling and Prediction

In 5G, wireless traffic prediction is vital to resource allocation, load-aware management, and proactive control in C-RAN. In [11], we considered a distributed GP based wireless traffic modeling and prediction that exploits the advanced C-RAN specifying the second network infrastructure given in the previous section. In the deployment area, several hundreds of micro base stations with fixed geographical positions are installed to serve mobile users and record the downlink physical resource block (PRB) usage (a wireless traffic usage indicator) versus time, namely a time series. These base stations are clustered

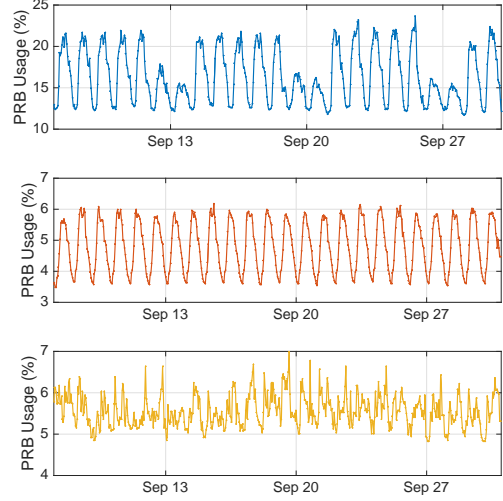


Fig. 11. The PRB usage curves of three base stations collected in three southern cities of China from September 1st to September 30th, 2015. The curve in the first panel represents one base station in an office area, where the traffic trend shows a strong weekly periodic pattern in accordance with weekdays and weekends. The curve in the second panel represents one base station in a residential area, which shows a strong daily pattern with higher demands in the daytime and lower demands in the nighttime. The curve in the third panel represents one base station in a rural area, where the data patterns are not obvious.

into groups according to their geographical locations and for each group a global aggregated PRB usage prediction model is to be built. To this end, all the micro base stations in one cluster send their own observed time series of PRB usage to an edge node, in which the data are aggregated, pre-processed and further uniformly allocated to a number of parallel computing units.

Specifically, a global GP regression model for the aggregated wireless traffic data of each cluster in the C-RAN is as follows:

$$y = f(t) + e, \quad (27)$$

where $y \in \mathbb{R}^1$ is a continuously valued scalar output representing the PRB usage; e is the independent noise, which is assumed to be Gaussian distributed with zero mean and variance σ_e^2 ; $f(t)$ is the regression function in terms of time modeled by a GP as introduced in Eq.(1) of Section 3.

As compared with deep learning black-box models such as recurrent neural network (RNN) and long-short term memory (LSTM), GP models have good interpretability as they are able to encode the prior information of the wireless traffic pattern into the kernel function design. The wireless traffic in the real data sets demonstrates the following general patterns: 1) *weekly periodic pattern*: the variation in accordance with

weekdays and weekends; 2) *daily periodic pattern*: the variation in accordance with weekdays and weekends; 3) *deviations*: small scale variation on top of the above periodic trends. We show a few examples in Fig. 11.

The FedLoc framework works as follows. First, each base station in a specific cluster uploads its measured time series to the locally-central node. The aggregated data is then divided by the edge node into K portions, and each portion is allocated to a local computing unit for distributed model training based on the cADMM introduced in Section 4. The training framework achieves excellent tradeoff between the communication overhead and training performance, as explained in Section 3. For each local computation unit, the computational complexity of training phase can be reduced from $\mathcal{O}(N^3)$ of the standard GP to $\mathcal{O}(\frac{N^3}{K^2})$, where N is the number of the data points and K is the number of parallel computing units.

In the online test phase, we could simply use the generalized PoE to fuse the local predictions from all parallel computing units to approximate the global prediction. The generalized PoE model needs to introduce a set of weight parameters $\beta_i, i = 1, 2, \dots, K$ to tune the importance of the local predictions. The resulting PoE predictive distribution is

$$p(f_*|\mathbf{x}_*, \mathcal{D}) \approx \prod_{i=1}^K p_i^{\beta_i}(f_*|\mathbf{x}_*, \mathcal{D}^{(i)}), \quad (28)$$

where β_i is the weight for the i -th local GP model and the corresponding posterior mean and variance are, respectively,

$$\mu_* = \sigma_*^2 \sum_{i=1}^K \beta_i \sigma_i^{-2}(\mathbf{x}_*) \mu_k(\mathbf{x}_*), \quad (29)$$

$$\sigma_*^2 = \left(\sum_{i=1}^K \beta_i \sigma_i^{-2}(\mathbf{x}_*) \right)^{-1}. \quad (30)$$

Consequently, the choice of β is vital to the prediction phase. In [11], we proposed to fuse the prediction results from local GP models elegantly via optimizing the fusion weights according to a cross-validation criterion. More specifically, we proved that the weight optimization problem can be solved efficiently with convergence guarantees. Besides, we also proposed a simplified fusion weight optimization method based on the soft-max function.

6.5. Other Applications

Due to space limitation, we are unable to introduce more use cases with great details. However, we list the following related use cases:

(1) *Radio feature map construction*. The proposed FedLoc framework can be used for a number of collaborating mobile users to build an accurate radio map, such as RSS map or magnetic field map, etc on each floor of a big building. In [60], we proposed a distributed recursive GP framework for

building indoor RSS maps. Therein, a batch of mobile users is assume to collected RSS measurements from various WiFi access points by walking in the deployed area independently. In the training phase, each mobile user then trains a local GP empowered RSS map individually, and in the inference phase a global prediction can be obtained by fusing all the local GP models via the classical Bayesian committee machine or its robust variant, rBCM. This work can be easily refined by fitting a global GP model in the training phase through using the ADMM introduced in Section 4 and using the optimal cross-validation based fusion strategy.

(2) *Simultaneous localization and mapping for 3D indoor scenario construction*. The proposed FedLoc framework can be used for a number of collaborating robots or low-flying UAVs equipped with cameras to reconstruct a 3D indoor scenario. A generic SLAM model [66] is given as follows:

$$\begin{aligned} \mathbf{x}_t &= f(\mathbf{x}_{t-1}, \mathbf{u}_{t-1}) + \mathbf{e}_{t-1}, \\ \mathbf{m}_t &= \mathbf{m}_{t-1}, \\ \mathbf{y}_t &= g(\mathbf{x}_t, \mathbf{m}_t, \mathbf{u}_t) + \mathbf{n}_t, \end{aligned} \quad (31)$$

where the dynamic motion model, f , has an additional inertial input \mathbf{u}_t to account for the sensory data from odometer, accelerometer, gyroscope, etc; there is an additional map memory state, \mathbf{m}_t , where the positions of the landmarks are updated and stored; the measurement model takes the updated map memory state as the input. We could potentially modify the GPSSM framework and let a bunch of mobile users or robots to perform the federated SLAM. Different from the use cases given in Section 6, federated SLAM imposes much higher requirements on both the computation power of the mobile devices and the data throughput (both uplink and downlink) of the network, when dealing with 3D environment reconstruction. The 5G network and futuristic wide-band generation (B5G or 6G) could help make the federated SLAM possible.

7. RESULTS

In this section, we show the effectiveness of the FedLoc framework with two examples evaluated using real data sets. In the first example, we adopt the GP model and mainly focus on the algorithmic effectiveness of the distributed model training of a small batch of hyper-parameters. In the second example, we adopt the DNN model and focus on practical implementation aspects.

7.1. GPSSM for Target Tracking

In this section, we will demonstrate one example of applying the federated learning framework for target tracking. The experimental setup is for ease of practical deployment of the framework, thus may not be optimal. Our focus is on both the training and prediction performance of the global, centralized model versus distributed implementations of it.

Due to space limitation, we will only show some primary results for the transition function in the GP-SSM. The model is $\mathbf{x}_{t+1} = f(\mathbf{x}_t) + \mathbf{e}_t$, where the vector $\mathbf{x}_t = [x_t, y_t]^T$ contains the 2-D position of a pedestrian at time instance t . We apply individual GPs for each dimension, namely, we let

$$x_{t+1} = f_x(\mathbf{x}_t) + e_{x,t}, \quad (32a)$$

$$y_{t+1} = f_y(\mathbf{x}_t) + e_{y,t}, \quad (32b)$$

where both $f_x(\mathbf{x}_t)$ and $f_y(\mathbf{x}_t)$ are represented as GP; for instance, we let

$$f_x(\mathbf{x}_t) \sim GP(m_x(\mathbf{x}_t), k_x(\mathbf{x}_t, \mathbf{x}_{t'})). \quad (33)$$

For clearer exposition, we let the mean function $m_x(\mathbf{x}_t)$ be zero and the kernel function $k_x(\mathbf{x}_t, \mathbf{x}_{t'})$ be an ARD kernel, more specifically,

$$k_x(\mathbf{x}_t, \mathbf{x}_{t'}) = \sigma_{s,x}^2 \exp \left[-\frac{(x_t - x_{t'})^2}{l_{xx}} - \frac{(y_t - y_{t'})^2}{l_{yy}} \right], \quad (34)$$

where the kernel hyper-parameters are $[\sigma_{s,x}^2, l_{xx}, l_{yy}]^T$. For the y -dimension, we adopt a similar ARD kernel, $k_y(\mathbf{x}_t, \mathbf{x}_{t'})$, but with different kernel hyper-parameters $[\sigma_{s,y}^2, l_{yx}, l_{yy}]^T$.

The above GP models can be trained globally with a training data set \mathcal{D} via the global, centralized maximum-likelihood estimation shown in Eq.(12). We know that the computational complexity scales as $\mathcal{O}(n^3)$ for centralized training. Using the FedLoc framework is beneficial. On the one hand, mobile users can collect their own local training data without worrying about the data leakage issue, which may well encourage more of them to collaborate. By adopting the cADMM or the pxADMM introduced in Section 4 to tune the model hyper-parameters in a distributed manner, the overall computational complexity can be reduced to $\mathcal{O}(n^3/K^3)$, where K is the number of collaborating mobile users. More specifically, this work can be seen as a collaborative, data-driven method for learning the human motion trajectory, which is important for us to understand and anticipate the behavior of human/smart agents and predict their future positions. A survey on other categories of methods can be found in [67].

To evaluate the performance of the FedLoc, we collected a real data set in a live indoor office environment. The data set contains more than 50 trajectories with around 25,000 samples. In the training phase, three mobile users each collected 15 trajectories. Each mobile user approximates the global GP model shown in Eq.(12) using only the local data, namely its own 15 trajectories. In the test phase, we use the model hyper-parameters trained from the FedLoc to perform posterior prediction of the next state given a novel current state.

We compare two distributed GP hyperparameter optimization schemes: 1) pxADMM with the regularization parameters $\rho_i = 500$ and $L_i = 5000, \forall i$; 2) cADMM with $\rho_i = 500$, for $i = 1, 2, 3$. Values for ρ_i and L_i are selected according to our previous experience on the two algorithms for other

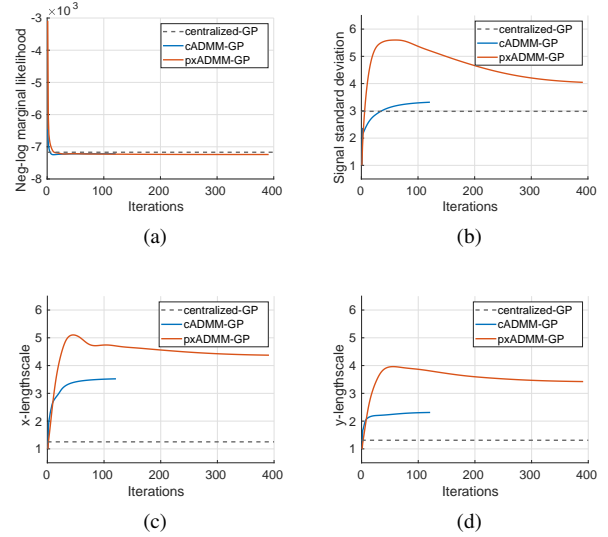


Fig. 12. For the GP modeling along the x -dimension, we show the negative log-marginal likelihood functions (centralized formulation refer to Eq.(12) and distributed formulation refer to Eq.(13)) in sub-figure (a); and the ARD kernel hyper-parameter estimates as a function of training iterations for the 3 input variables using pxADMM-GP and cADMM-GP in sub-figures (b-d) for model variance, length-scale in x , and length-scale in y , respectively.

data sets, therefore the setup is by no means optimal. Both the pxADMM and the cADMM use the same initialization, namely, the length scales, l , and variance, σ_s^2 are all set equal to 1. The program will be terminated when the difference in all optimization variables between two consequent iterations is within 10^{-3} . The computer program was implemented using MATLAB and executed on a computing server with 24 CPU cores (2.2 GHz) and 128 GB RAM.

We show the model training results for both dimensions x and y in Fig. 12 and Fig. 13. It is not surprising to see that the distributed programs converge to different model hyper-parameter estimates as compared to the ones trained centrally for the global model. One reason is that the distributed program uses a different cost function as shown in Eq.(13), which corresponds to reducing the kernel matrix $K(\mathbf{X}, \mathbf{X}; \boldsymbol{\theta})$ with only three main diagonal blocks left. Despite the difference in the hyper-parameter estimates, the corresponding negative log-marginal likelihood values as well as the overall prediction root-mean-squared-error (RMSE in meters) are fairly close. For the two distributed programs, namely the cADMM and the pxADMM, they also seem to converge to different stationary points for certain parameters as shown in the figures. But similarly, the negative log-marginal likelihood values as well as the overall prediction mean-squared-error (MSE) are fairly close. One possible reason might be that there exist various "not-bad" local minimal that to lead to similar objective and generaliza-

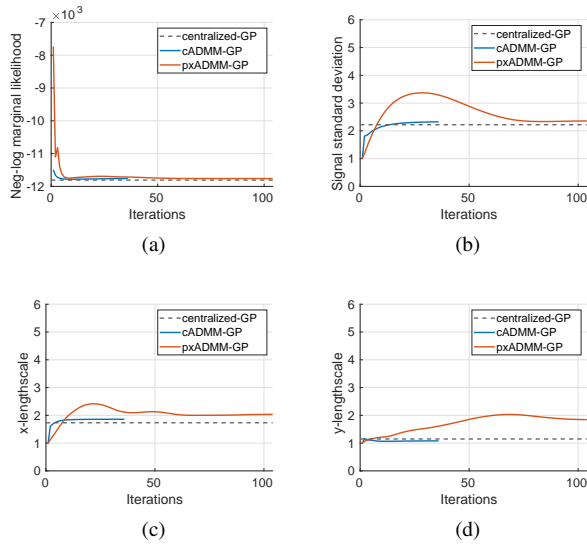


Fig. 13. Results for the GP modeling along the y -dimension.

Table 2. Comparisons between two distributed training programs with the centralized training program of the GP model.

	pxADMM-GP	cADMM-GP	centralized GP
RMSE	0.1368m	0.1353m	0.1313m
CT	714s	10838s	50000s

tion error of the trained model. From the computational time (CT) shown in Table 2, we observed that the pxADMM-GP scheme spends the least computational time. The pxADMM-GP scheme circumvents the rigorous and frequent gradient synchronization step by nature. This is because the closed-form proximal step w.r.t. local hyperparameters requires the time-consuming matrix inversion to be computed only once, resulting in a computationally efficient scheme.

7.2. Smart Navigation with Low-Sampling-Rate GPS

In this section, we will demonstrate the application of federated learning with DNN models for smart vehicle navigation with low-sampling-rate GPS, which has been described as one of the representative use cases in section 6.2. In this subsection, we will further show some primary results due to space limitation, while more details about this work can be found in our recent paper [Ref].

We start with introducing the implementation setups of our new proposed federated learning empowered navigation system prototype. First, real data sets (for both training and test) were collected by three collaborating users with their own private car driving on the campus of the Chinese University of Hong Kong (Shenzhen), see Fig. 14. During the data collection process, each car was equipped with a smart phone (Xiaomi), facing upwards and heading to the moving direction of the car.



Fig. 14. The map of CUHK(SZ), where we collected the real data.

The sensor data are then uploaded to the server through WiFi on the fly. These three collaborating users traveled around the campus and collected a total number of twelve trajectories of smart phone sensor data that contain real-time motion information of the vehicle. For each trajectory, the length of the data record may range from a few minutes to dozens of minutes. Therefore, the data tend to be non-i.i.d. across different users, because they own different number of trajectories collected on different routes.

After all training data sets have been collected, we adopted the federated learning framework to train the two DNNs for calibrating the sensor data, one for the velocity and the other one for the yaw angle, so that accurate navigation can be obtained even with low-sampling-rate GPS signals in the test phase/online phase. DNNs with five hidden layers (3000-3000-2000-1000-500) are selected as the global model in our prototype, which can be replaced with more sophisticated models for high-dimensional time series, such as LSTM. The input is the sensor data in a specific time window with dimension 600 for the first DNN or with dimension 401 for the second DNN, while the output is a scalar. In the training phase, the global model is updated by the three collaborating users through federated learning described in Algorithm 1. Specifically, we tried two different model training algorithms, namely the FedAve algorithm and the FedProx algorithm introduced in the previous section. We set the learning rate of both the FedAve and FedProx to be 10^{-4} . For the FedProx algorithm, the additional regularization parameter is set to 10^{-2} .

We show the training performance of both the FedAvg and the FedProx algorithms in Fig. 15. Both algorithms can achieve a very low training loss after a certain number of epochs. Meanwhile, we can observe that the FedProx algorithm demonstrates a smoother, more stable, but slower convergence profile than that of the FedAve algorithm, which well falls in our expectation owing to the additional proximal term

introduced into the FedProx algorithm. The reason is that the FedProx algorithm needs to balance between the training loss and the difference between the global model and the local models, thus avoiding significant change of the global model in any specific epoch and achieving a more smooth convergence curve at the cost of a slower convergence rate as compared with the FedAve.

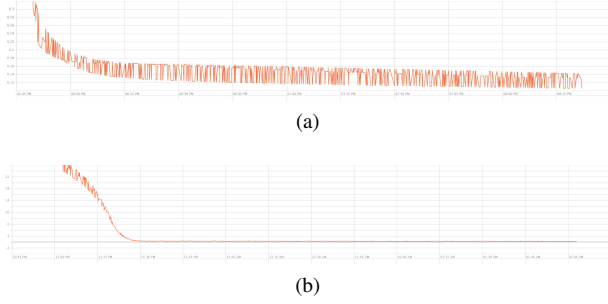


Fig. 15. Training loss versus epochs of the FedAve in comparison with the FedProx. (a) FedAve; (b) FedProx.

Lastly, we test the trained global learning model with two trajectories that are not used in the training phase. The GPS reference signals are only available for every 60 seconds, being much less frequent than the default setup (1 sample per second). During the time where there is no GPS signal available, the trained global learning models are used to calibrate the observed sensor data. We show the test results in Fig. 16. The navigation RMSE of the FedAvg being around 20 meters outperforms that of the FedProx in our simulations, despite of the fact that the FedProx algorithm shows a more stable and smoother training dynamic with epochs. Fine-tuning the learning rate of the FedProx algorithm may further improve its generalization performance. Nevertheless, using either the FedAvg algorithm or the FedProx algorithm leads to well improved navigation RMSE as compared to solely using the IMU for navigation with the RMSE being around 120 meters in our simulations.

8. FUTURE DIRECTIONS AND CHALLENGES

Potential challenges to the federated wireless localization are the following:

- An essential ingredient of the federated wireless localization framework is the mobile terminals. To ensure that the whole framework works smoothly, the mobile terminals should be able to process a modest amount of data and perform analysis with TensorFlow, PyTorch, etc. This requires further development of powerful but compressed deep learning models, mobile AI chips, etc. Advanced WiFi or 5G technologies nowadays can fulfill the requirement of communications between the mobile terminals and the central node. However, communication efficiency is a critical issue that requires further

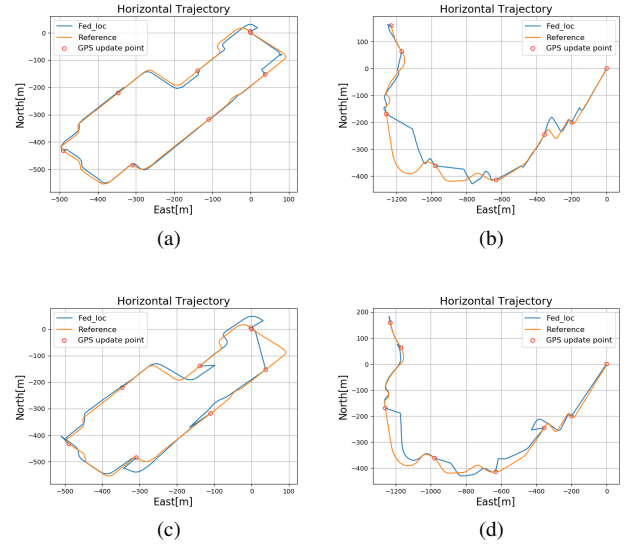


Fig. 16. The test performance on two different routes provided by the two algorithms. (a) and (b) for the FedAve algorithm; (c) and (d) for the FedProx algorithm.

treatment. In addition, an agreement on the standard protocol for synchronizing the mobile terminals is to be made. Interested readers may refer to a most recent work [68] discussed how to a scalable production system for Federated Learning with abundant system design details.

- In section 3, we mentioned that using DNN as the learning model will cause a lot of model parameters or their gradients to be communicated over the air. A more straightforward and practical way to reduce the communication burden is to quantize the DNN weights from 64 bits precision to 8 bits precision or even lower. In the context of distributed optimization, a signSGD method was proposed in [69] that quantizes every gradient update to its binary sign thus reducing the communication load by a factor of 32. However, Better understandings on the converge properties of such methods under more general federated learning setup, such as non-i.i.d. data distribution and imbalanced data amount over mobile users, need to be built.
- The federated learning framework requires mobile users to cooperate. However, there might be the case that some voluntary mobile users are malicious or careless with their shared messages. A promising way to solve such issues from the algorithmic perspective is to use robust distributed optimization and fusion techniques.
- For learning based wireless localization, the output data are mostly positions or position-related measures, which are more private to the collaborating users. The resulting

framework should be flexible so that the mobile users can choose whether to contribute their data labels (i.e. the outputs) or not. To this end, we could adopt semi-supervised learning models, which can handle data set with a big fraction of missing labels.

- So far, we have implicitly assumed that all the mobile users have sufficient number of local data for updating the global model hyper-parameters. This may not be true for voluntary users with very limited amount of data collected during the day. But the population of the voluntary users may well exceed that of the paid workers. To make use of these data, a trustful third party could be employed in edge clouds to aggregate data from different mobile users, as described in our second network infrastructure. Another way to alleviate this “small data” difficulty, from algorithmic perspective, is to harness the known canonical parametric model to generate virtual data and mix them with the limited amount of real data before training the model. In this way, we also transfer the prior knowledge of the canonical models to the eventual data-driven learning based model [70].
- We have talked exclusively about wireless localization. Actually, visual-based localization and target tracking have also attracted a lot of attention these days. The combination of wireless measurements and visual measurements would definitely improve the localization accuracy even further. For instance, in [71] wireless positioning was adopted in visual trackers to alleviate visual tracking pains, such as long-term tracking, feature model drifting, recovery. Their combination is a key enabler for autonomous driving and other robotic applications. However, their combination makes the data structure even more inhomogeneous for the federated learning to work properly.
- One could utilize mobile users social relationship to find more participants to join the learning process and improve the activeness of current participants. In this case, the popular graph learning techniques, e.g., graph GP, can serve as a promising learning module to enable efficient learning from graph-like structured dataset.

9. CONCLUSION

In this work, we proposed a new-fashioned collaboration framework for large-scale, data-driven learning-based wireless localization. It is called the federated wireless localization framework simply because we use the recently proposed federated learning framework to ensure that mobile users collaborate with privacy preservation. The algorithmic core of the federated learning is fairly similar to some prior art, for instance, the consensus algorithm and the ADMM. We think it is the right time to bring up this federated wireless localization

framework due to the following reasons. First, high-precision wireless localization is desperately demanded, which can be achieved by combining an empirical model with a large-scale data driven model. Second, the calibration of a localization method consumes a lot of time and workforce. Collaboration among mobile users can largely facilitate the calibration work. Third, smartphones are becoming a powerful platform for computational demands. Fourth, we have seen rapid development in large-scale optimization techniques, 5G communication networks, data compression and encryption, among other techniques. Prototypes will be seen in the near future undoubtedly.

Acknowledgement

The authors would like to thank the visiting students Ang Xie and Wenbiao Guo from Beijing Jiaotong University for preparing some simulation results and references.

10. REFERENCES

- [1] C. E. Rasmussen and C. I. K. Williams, *Gaussian Processes for Machine Learning*, vol. 1, Cambridge, MA, USA: MIT Press, 2006.
- [2] B. McMahan, E. Moore, D. Ramage, S. Hampson, and B. Aguera y Arcas, “Communication-efficient learning of deep networks from decentralized data,” in *Proc. Int. Conf. Artif. Intell. Stat. (AISTATS)*, Fort Lauderdale, FL, USA, Apr. 2017, pp. 1273–1282.
- [3] D. Povey, X. Zhang, and S. Khudanpur, “Parallel training of deep neural networks with natural gradient and parameter averaging,” in *Proc. Int. Conf. Learn. Represent. (ICLR) Workshop*, San Diego, CA, USA, May 2015.
- [4] N. Neverova, C. Wolf, G. Lacey, L. Fridman, D. Chandra, B. Barbello, and G. Taylor, “Learning human identity from motion patterns,” *IEEE Access*, vol. 4, pp. 1810–1820, Apr. 2016.
- [5] N. H. Tran, W. Bao, A. Zomaya, Nguyen M. NH, and C. S. Hong, “Federated learning over wireless networks: Optimization model design and analysis,” in *Proc. IEEE INFOCOM*, Paris, France, Apr. 2019, pp. 1387–1395.
- [6] S. Samarakoon, M. Bennis, W. Saad, and M. Debbah, “Federated learning for ultra-reliable low-latency V2V communications,” in *Proc. IEEE Glob. Commun. Conf. (GLOBECOM)*, Abu Dhabi, United arab emirates, Dec. 2018, pp. 1–7.
- [7] J. Lee, J. Sun, F. Wang, S. Wang, C-H Jun, and X. Jiang, “Privacy-preserving patient similarity learning in a federated environment: development and analysis,” *JMIR Med. Inform.*, vol. 6, no. 2, pp. e20, 2018.

- [8] F. Gustafsson and F. Gunnarsson, "Mobile positioning using wireless networks: possibilities and fundamental limitations based on available wireless network measurements," *IEEE Signal Process. Mag.*, vol. 22, no. 4, pp. 41–53, June 2005.
- [9] A. H. Sayed, A. Tarighat, and N. Khajehnouri, "Network-based wireless location: challenges faced in developing techniques for accurate wireless location information," *IEEE Signal Process. Mag.*, vol. 22, no. 4, pp. 24–40, July 2005.
- [10] Y. Bar-Shalom, X.-R. Li, and T. Kirubarajan, *Estimation with Applications to Tracking and Navigation*, John Wiley & Sons, Inc., New York, NY, 2001.
- [11] Y. Xu, F. Yin, W. Xu, J. Lin, and S. Cui, "Wireless traffic prediction with scalable Gaussian process: Framework, algorithms, and verification," *IEEE J. Sel. Areas Commun.*, vol. 37, no. 6, pp. 1291–1306, June 2019.
- [12] L. Liu, Z. Qiu, G. Li, Q. Wang, W. Ouyang, and L. Lin, "Contextualized spatial-temporal network for taxi origin-destination demand prediction," *IEEE Trans. Intell. Transp. Syst.*, vol. 20, no. 10, pp. 3875–3887, May 2019.
- [13] TY Kim and SB Cho, "Predicting residential energy consumption using CNN-LSTM neural networks," *Energy*, vol. 182, pp. 72–81, Sept. 2019.
- [14] Z. Qi, T. Wang, G. Song, W. Hu, X. Li, and Z. Zhang, "Deep air learning: Interpolation, prediction, and feature analysis of fine-grained air quality," *IEEE Trans. Knowl. Data Eng.*, vol. 30, no. 12, pp. 2285–2297, Apr. 2018.
- [15] N. Patwari, J. N. Ash, S. Kyperountas, A. O. Hero III, R. L. Moses, and N. S. Correal, "Locating the nodes: cooperative localization in wireless sensor networks," *IEEE Signal Process. Mag.*, vol. 22, no. 4, pp. 54–69, Jul. 2005.
- [16] P. Biswas, T.-C. Lian, T.-C. Wang, and Y. Ye, "Semidefinite programming based algorithms for sensor network localization," *ACM Trans. Sen. Netw.*, vol. 2, no. 2, pp. 188–220, May 2006.
- [17] H. Wymeersch, J. Lien, and M. Z. Win, "Cooperative localization in wireless networks," *Proc. IEEE*, vol. 97, no. 2, pp. 427–450, Feb. 2009.
- [18] N. Patwari, A. O. Hero III, M. Perkins, N. S. Correal, and R. J. O'Dea, "Relative location estimation in wireless sensor networks," *IEEE Trans. Signal Process.*, vol. 51, no. 8, pp. 2137–2148, Aug. 2003.
- [19] F. Yin, C. Fritsche, D. Jin, F. Gustafsson, and A. M. Zoubir, "Cooperative localization in WSNs using Gaussian mixture modeling: Distributed ECM algorithms," *IEEE Trans. Signal Process.*, vol. 63, no. 6, pp. 1448–1463, Mar. 2015.
- [20] C. Wu, Z. Yang, and Y. Liu, "Smartphones based crowdsourcing for indoor localization," *IEEE Trans. Mobile Comput.*, vol. 14, no. 2, pp. 444–457, Feb. 2015.
- [21] C. Zhang, K. P. Subbu, J. Luo, and J. Wu, "GROPING: Geomagnetism and crowdsensing powered indoor navigation," *IEEE Trans. Mobile Comput.*, vol. 14, no. 2, pp. 387–400, Feb. 2015.
- [22] K. Hornik, "Approximation capabilities of multilayer feedforward networks," *Neural Networks*, vol. 4, no. 2, pp. 251–257, 1991.
- [23] S. Theodoridis, *Machine Learning: a Bayesian and Optimization Perspective*, Academic Press, 2015.
- [24] I. Goodfellow, Y. Bengio, and A. Courville, *Deep Learning*, Cambridge, MA, USA: MIT Press, 2016.
- [25] A. G. Wilson and R. P. Adams, "Gaussian process kernels for pattern discovery and extrapolation," in *Proc. Int. Conf. Mach. Learn. (ICML)*, Atlanta, USA, July 2013, pp. 1067–1075.
- [26] F. Yin, X. He, L. Pan, T. Chen, Z.-Q. Luo, and S. Theodoridis, "Sparse structure enabled grid spectral mixture kernel for temporal Gaussian process regression," in *Proc. Int. Conf. Inf. Fusion (FUSION)*, Cambridge, UK, July 2018, pp. 47–54.
- [27] A. G. Wilson, Z. Hu, R. Salakhutdinov, and E. P. Xing, "Deep kernel learning," in *Proc. Int. Conf. Artif. Intell. Stat. (AISTATS)*, Cadiz, Spain, May 2016, pp. 370–378.
- [28] A. Damianou and N. Lawrence, "Deep Gaussian processes," in *Proc. Int. Conf. Artif. Intell. Stat. (AISTATS)*, Scottsdale, AZ, USA, Apr. 2013, pp. 207–215.
- [29] A. Matthews, J. Hron, M. Rowland, R. E. Turner, and Z. Ghahramani, "Gaussian process behaviour in wide deep neural networks," in *Proc. Int. Conf. Learn. Represent. (ICLR)*, Vancouver, BC, Canada, Apr. 2018.
- [30] J. Lee, J. Sohl-dickstein, J. Pennington, R. Novak, S. Schoenholz, and Y. Bahri, "Deep neural networks as Gaussian processes," in *Proc. Int. Conf. Learn. Represent. (ICLR)*, Vancouver, BC, Canada, Apr. 2018.
- [31] R. M. Neal, *Bayesian Learning for Neural Networks*, Ph.D. thesis, University of Toronto, Canada, 1995.
- [32] Y. Cho and L. K. Saul, "Kernel methods for deep learning," in *Proc. Adv. Neural Inf. Process. Syst. (NeurIPS)*, Vancouver, BC, Canada, Dec. 2009, pp. 342–350.
- [33] A. Jacot, F. Gabriel, and C. Hongler, "Neural tangent kernel: Convergence and generalization in neural networks," in *Proc. Adv. Neural Inf. Process. Syst. (NeurIPS)*, Montreal, Canada, Dec. 2018, pp. 8571–8580.

- [34] S. Arora, SS Du, W. Hu, Z. Li, RR Salakhutdinov, and R. Wang, "On exact computation with an infinitely wide neural net," in *Proc. Adv. Neural Inf. Process. Syst. (NeurIPS)*, Vancouver, BC, Canada, Dec. 2019, pp. 8139–8148.
- [35] M. Belkin, D. Hsu, S. Ma, and S. Mandal, "Reconciling modern machine learning practice and the bias-variance trade-off," *arXiv preprint arXiv:1812.11118v2*, 2019.
- [36] G. Hinton, O. Vinyals, and J. Dean, "Distilling the knowledge in a neural network," *arXiv preprint arXiv:1503.02531v1*, 2015.
- [37] J. Frankle and M. Carbin, "The lottery ticket hypothesis: Finding sparse, trainable neural networks," in *Proc. Int. Conf. Learn. Represent. (ICLR)*, New Orleans, LA, USA, May 2019.
- [38] A. Girard, *Approximate Methods for Propagation of Uncertainty with Gaussian Process Model*, Ph.D. thesis, University of Glasgow, Glasgow, UK, 2004.
- [39] C. Bishop, *Machine Learning and Pattern Recognition*, New York, USA: Springer, 2006.
- [40] Simo Särkkä, *Bayesian Filtering and Smoothing*, Cambridge University Press, 2013.
- [41] J. Konečný, H. McMahan, X. Yu, P. Richtárik, A. Suresh, and D. Bacon, "Federated learning: Strategies for improving communication efficiency," *arXiv preprint arXiv:1610.05492*, 2016.
- [42] M. P. Deisenroth and J. W. Ng, "Distributed Gaussian processes," in *Proc. Int. Conf. Mach. Learn. (ICML)*, Lille, France, July 2015, pp. 1481–1490.
- [43] S. Boyd, N. Parikh, E. Chu, B. Peleato, and J. Eckstein, "Distributed optimization and statistical learning via the alternating direction method of multipliers," *Found. Trends Mach. Learn.*, vol. 3, no. 1, pp. 1–122, Jan. 2011.
- [44] M. Hong, Z.-Q. Luo, and M. Razaviyayn, "Convergence analysis of alternating direction method of multipliers for a family of nonconvex problems," *SIAM J. Optimiz.*, vol. 26, no. 1, pp. 337–364, Jan. 2016.
- [45] A. K. Sahu, T. Li, M. Sanjabi, M. Zaheer, A. Talwalkar, and V. Smith, "On the convergence of federated optimization in heterogeneous networks," *arXiv preprint arXiv:1812.06127*, 2018.
- [46] Q. Yang, Y. Liu, T. Chen, and Yong Tong, "Federated machine learning: Concept and applications," *ACM Trans. Intell. Syst. Technol.*, vol. 10, no. 2, pp. 492–503, Feb. 2019.
- [47] Eiman Mohyeldin, "Minimum technical performance requirements for imt-2020 radio interface(s)," https://www.itu.int/en/ITU-R/study-groups/rsg5/rwp5d/imt-2020/Documents/S01-1_Requirements%20for%20IMT-2020_Rev.pdf, 2020.
- [48] "3gpp release 10," <https://www.3gpp.org/specifications/releases/70-release-10>, 2013.
- [49] "IEEE draft standard for information technology – telecommunications and information exchange between systems local and metropolitan area networks – specific requirements part 11: Wireless lan medium access control (mac) and physical layer (phy) specifications amendment enhancements for high efficiency wlan," *IEEE P802.11ax/D6.0*, November 2019, pp. 1–780, Dec 2019.
- [50] "IEEE standard for information technology– telecommunications and information exchange between systems local and metropolitan area networks– specific requirements–part 11: Wireless lan medium access control (mac) and physical layer (phy) specifications–amendment 4: Enhancements for very high throughput for operation in bands below 6 ghz.," *IEEE Std 802.11ac-2013 (Amendment to IEEE Std 802.11-2012, as amended by IEEE Std 802.11ae-2012, IEEE Std 802.11aa-2012, and IEEE Std 802.11ad-2012)*, pp. 1–425, Dec 2013.
- [51] F. Gustafsson and F. Gunnarsson, "Measurements used in wireless sensor networks localization," in *Localization Algorithms and Strategies for Wireless Sensor Networks: Monitoring and Surveillance Techniques for Target Tracking*, pp. 33–53. IGI Global, Hershey, PA, USA, 2009.
- [52] F. Yin, Y. Zhao, and F. Gunnarsson, "Proximity report triggering threshold optimization for network-based indoor positioning," in *Proc. Int. Conf. Inf. Fusion (FUSION)*, Washington, DC, USA, July 2015, pp. 1061–1069.
- [53] J. Liu, N. Liu, Z. Pan, and X. You, "Autloc: Deep autoencoder for indoor localization with RSS fingerprinting," in *2018 10th International Conference on Wireless Communications and Signal Processing (WCSP)*, Hangzhou, China, Oct 2018, pp. 1–6.
- [54] C. Hsieh, J. Chen, and B. Nien, "Deep learning-based indoor localization using received signal strength and channel state information," *IEEE Access*, vol. 7, 2019.
- [55] J. Qi, H. Li, F. Yin, B. Ai, and S. Cui, "Navigation with low-sampling-rate GPS and smartphone sensors: A data-driven learning-based approach," in *International Conference on Wireless, Mobile and Multimedia Networks (ICWMMN)*, Beijing, China, Nov. 2019, pp. 1–6.

- [56] T. Schön, A. Wills, and B. Ninness, “System identification of nonlinear state-space models,” *Automatica*, vol. 47, no. 1, pp. 39–49, Jan. 2011.
- [57] C. Andrieu, A. Doucet, and R. Holenstein, “Particle Markov chain Monte Carlo methods,” *J. Roy. statistical Soc. B-Stat. Method.*, vol. 72, no. 3, pp. 269–342, June 2010.
- [58] R. Frigola, Y. Chen, and C. E. Rasmussen, “Variational Gaussian process state-space models,” in *Proc. Adv. Neural Inf. Process. Syst. (NeurIPS)*, Montreal, Canada, Dec. 2014, pp. 3680–3688.
- [59] Y. Zhao, F. Yin, F. Gunnarsson, F. Hultkratz, and J. Fagerlind, “Gaussian processes for flow modeling and prediction of positioned trajectories evaluated with sports data,” in *Proc. Int. Conf. Inf. Fusion (FUSION)*, Heidelberg, Germany, July 2016, pp. 1461–1468.
- [60] F. Yin and F. Gunnarsson, “Distributed recursive Gaussian processes for RSS map applied to target tracking,” *IEEE J. Sel. Topics Signal Process.*, vol. 11, no. 3, pp. 492–503, Apr. 2017.
- [61] A. Xie, F. Yin, B. Ai, and S. Cui, “A real indoor navigation system based on variational Gaussian process state-space model and smartphone sensory data,” *arXiv preprint arXiv:1910.10773*, 2019.
- [62] Y. Zhao, C. Fritsche, F. Yin, and F. Gunnarsson, “Cramer-rao bounds for filtering based on Gaussian process state-space models,” *IEEE Trans. Signal Process.*, vol. 67, no. 23, pp. 5936–5951, Dec. 2019.
- [63] A. D. Ialongo, M. van der Wilk, and C. E. Rasmussen, “Closed-form inference and prediction in Gaussian process state-space models,” in *Proc. Adv. Neural Inf. Process. Syst. (NeurIPS) Time Series Workshop*, Long Beach, California, USA, Dec. 2017.
- [64] M. K. Titsias, “Variational learning of inducing variables in sparse Gaussian processes,” in *Proc. Int. Conf. Artif. Intell. Stat. (AISTATS)*, Clearwater Beach, Florida, USA, Apr. 2009, pp. 567–574.
- [65] Y. Gal, M. van der Wilk, and C. E. Rasmussen, “Distributed variational inference in sparse Gaussian process regression and latent variable models,” in *Proc. Adv. Neural Inf. Process. Syst. (NeurIPS)*, Montreal, Canada, Dec. 2014, pp. 3257–3265.
- [66] F. Gustafsson, *Statistical Sensor Fusion*, Studentlitteratur, Lund, Sweden, 2012.
- [67] A. Rudenko, L. Palmieri, M. Herman, K. M. Kitani, D. M. Gavrila, and K. O. Arras, “Human motion trajectory prediction: A survey,” *arXiv preprint arXiv:1905.06113*, 2019.
- [68] K. Bonawitz, H. Eichner, W. Grieskamp, and D. Huba et.al., “Towards federated learning at scale: System design,” *arXiv preprint arXiv:1902.01046*, 2019.
- [69] J. Bernstein, Y-X Wang, K. Azizzadenesheli, and A. Anandkumar, “signSGD: Compressed optimisation for non-convex problems,” *arXiv preprint arXiv:1802.04434*, 2018.
- [70] A. Zappone, M. Di Renzo, M. Debbah, T. T. Lam, and X. Qian, “Model-aided wireless artificial intelligence: Embedding expert knowledge in deep neural networks for wireless system optimization,” *IEEE Veh. Technol. Mag.*, vol. 14, no. 3, pp. 60–69, Sept. 2019.
- [71] P. Hu, Z. Yan, R. Huang, and F. Yin, “How effectively can indoor wireless positioning relieve visual tracking pains: A Cramer-Rao bound viewpoint,” in *Proc. IEEE Int. Conf. Image Process. (ICIP)*, Taipei, Taiwan, Sept. 2019, pp. 3083–3087.